UC San Diego
UC San Diego Previously Published Works

Title

Osmium isotope evidence for a heterogeneous 3He/4He mantle plume beneath the Juan Fernandez Islands

Permalink

https://escholarship.org/uc/item/6z76t96h

Authors

Paquet, Marine
Day, James MD
Castillo, Paterno R

Publication Date

2019-09-01

DOI

10.1016/j.gca.2019.06.039

Peer reviewed

Osmium isotope evidence for a heterogeneous ³He/⁴He mantle plume beneath the Juan Fernandez Islands

Marine Paquet [*], James M.D. Day, Paterno R. Castillo

Scripps Institution of Oceanography, University of California San Diego, La Jolla, CA 92093, USA

Abstract

Mantle plume models have been widely applied to explain the formation of ocean island basalts (OIB), with high-³He/⁴He in their lavas being explained by sampling of a primitive deep mantle source. The Juan Fernandez Islands have ³He/⁴He (7.8–18 R_A) similar to or higher than in mid-ocean ridge basalts (MORB; 8 ± 1 R_A) and have been used to both support and refute the mantle plume hypothesis. Ambiguity regarding the origin of the Juan Fernandez Islands primarily originates from interpretation of mantle source signatures between the lava series from the two main islands, Robinson Crusoe and Alexander Selkirk. To examine this issue, we report new whole-rock and olivine separate ¹⁸⁷Os/¹⁸⁸Os ratios and major-, trace-, and highly siderophile-element (HSE: Re, Pd, Pt, Ru, Ir, Os) abundances. The HSE and trace element abundances in Juan Fernandez main shield lavas can be explained by up to 30% olivine removal, together with spinel crystallization at 1–5 kbar, whereas Robinson Crusoe rejuvenated lavas can be reproduced by higher-pressure fractional crystallization (up to 10 kbar). An assemblage of 30 modal % olivine and 1–5 modal % spinel, combined with the additional contribution of primary melt trapped in olivine inclusions reproduces the range of HSE compositions observed in Juan Fernandez Archipelago olivine grains. Ratios of ¹⁸⁷Os/¹⁸⁸Os for Juan Fernandez lavas are generally less radiogenic than global OIB and show no correlation with indices of fractionation, indicating that they reflect mantle source compositions. Younger basanite lavas from Robinson Crusoe represent rejuvenated volcanism dominantly from a depleted lithospheric mantle source (¹⁸⁷Os/¹⁸⁸Os < 0.13) mixed with a high-³He/⁴He component from the main shield building stage. These lavas are similar in origin and composition to other Pacific rejuvenated lavas (e.g., Samoa, Hawaii). Robinson Crusoe main shield lavas are from a high-³He/⁴He (>18 R_A) and enriched mantle source (¹⁸⁷Os/¹⁸⁸Os = 0.1312) similar to the 'C' or 'FOZO' component, whereas Alexander Selkirk lavas are consistent with a dominant contribution from a depleted, low-³He/⁴He (<10 R_A) mantle component. The mantle sources of the shield lavas yield subtle variations in Sr-Nd-Os-Pb isotope space and have no clear variations with relative or absolute abundances of the HSE or trace elements. These results are consistent with a heterogeneous mantle plume model, with initial eruption of lavas from a primitive high-³He/⁴He mantle source ∼4 million years ago (Ma) to form Robinson Crusoe Island, which also led to ³He enrichment of the oceanic lithosphere, followed by eruption of Alexander Selkirk lavas from a more depleted mantle source at ∼2 Ma. Juan Fernandez lavas show that mantle heterogeneity preserved in OIB can occur over short-timescales (<2 Ma) and can impact lithospheric compositions, leading to eruption of rejuvenated lavas with unusual isotopic characteristics.

---

* Corresponding author.

E-mail address: mpaquet@ucsd.edu (M. Paquet).

1. INTRODUCTION

Ocean island basalts (OIB) with high $^3He/^4He$ ratios (e.g., Hawaii, Iceland, Galapagos, Samoa, Réunion and the Juan Fernandez Islands) are widely considered to originate from primordial lower mantle via upwelling plumes (e.g. Kurz et al., 1982; Hart et al., 1992; Farley et al., 1992). Hence, these high-$^3He/^4He$ OIB are probes to better constrain the composition of the deep mantle. High-$^3He/^4He$ lavas are linked to conventional radiogenic isotope systematics in that they converge to a common mantle component in Sr-Nd-Pb isotope space, variably called FOZO (Focus Zone: Hart et al., 1992), PHEM (Primitive Helium Mantle: Farley et al., 1992), or C (Common: Hanan and Graham, 1996), which only differ in detail from their isotope compositions in Sr, Nd and Pb isotopes, if at all (Hofmann, 2014).

The Juan Fernandez volcanic chain in the southeastern Pacific is an important location for investigating geochemical variations in OIB in so far as its lavas show a large range of $^3He/^4He$ compositions, between 7.8 and 18.0 R_A ($^3He/^4He$ normalized to air; Farley et al., 1993), from normal MORB-like ratios (8 ± 1 R_A; Graham, 2002) to higher ratios, which have previously been interpreted as a deep-mantle source signature (e.g. Kurz et al., 1982; Hart et al., 1992). In contrast to their variable He isotope compositions, Juan Fernandez lavas span a limited range of Sr-Nd-Pb isotope ratios (Gerlach et al., 1986; Baker et al., 1987; Farley et al., 1993; Truong et al., 2018). The Juan Fernandez volcanic island and seamount chain is located at 34°S on the Nazca Plate, between 76° and 83°W, approximately 660 km west of Chile (Fig. 1). The chain is composed of two main islands, 180 km apart from each other, Robinson Crusoe (also called Mas a Tierra, closer to the land, at approximately 78°50′W), and Alexander Selkirk (Mas Afuera, away from the land, at approximately 80° 50′W). A small island, Santa Clara, to the southwest of Robinson Crusoe, and numerous seamounts rise along the aseismic ridge oriented east-west at 34°S (Baker et al., 1987; Farley et al., 1993; Devey et al., 2000; Rodrigo and Lara, 2014; Lara et al., 2018a, 2018b). Radiometric ($^{40}Ar/^{39}Ar$) ages for shield lavas range between 8.41–9.26 Ma for O'Higgins Guyot (e.g. Lara et al., 2018b), 3.40–4.10 Ma for Robinson Crusoe Island (Reyes et al., 2017; Lara et al., 2018b), and 0.83–0.94 Ma for Alexander Selkirk Island (Lara et al., 2018b). Previous studies reported K-Ar ages up to 5.8 ± 2.1 Ma for Santa Clara, from 3.1 ± 0.9 to 4.2 ± 0.2 Ma for Robinson Crusoe, and from 0.85 ± 0.3 Ma to 2.4 ± 0.1 Ma for Alexander Selkirk (Booker et al., 1967; Stuessy et al., 1984; Baker et al., 1987). All available age data suggest a difference between Robinson Crusoe and Alexander Selkirk Islands of ∼2 to 3 Ma, which is in good agreement with the Nazca Plate moving eastward at a spreading rate of about 74 mm·yr^{-1} (DeMets et al., 2010). Previous studies described fresh basalts from Friday and Domingo seamounts (Farley
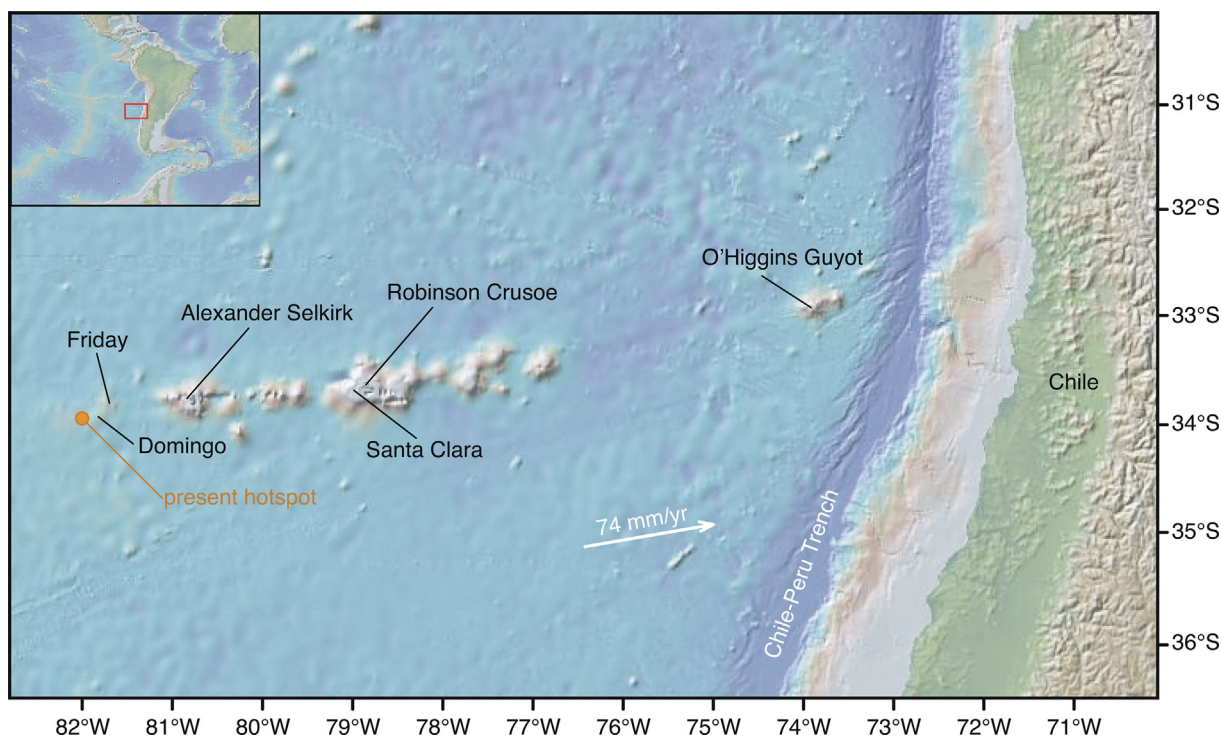

Fig. 1. Juan Fernandez Ridge (figure modified from Lara et al., 2018b; map downloaded from www.GeoMapApp.com). The white arrow corresponds to the present day displacement of the Nazca Plate relative to South America (DeMets et al., 2010). O'Higgins Guyot, Santa Clara, Robinson Crusoe Island and Alexander Selkirk Island show $^{40}Ar/^{39}Ar$ ages of 8.41–9.26 Ma, 4.58–4.63 Ma, ∼3.40–4.10 Ma and ∼0.83–0.94 Ma respectively (e.g. Reyes et al., 2017; Lara et al., 2018a, 2018b). The location of the present hotspot is inferred from the age progression defined by Ar ages (Lara et al., 2018b).

et al., 1993; Devey et al., 2000), indicating that these seamounts are younger than Alexander Selkirk. The progressively younger ages to the west support the hypothesis of an age-progressive hotspot volcanism.

Early studies argued that the eastward movement of the Nazca Plate over a stationary plume formed the Juan Fernandez volcanic chain, making new volcanoes in the west while the magma supply to the older volcanoes was decreasing (Baker et al., 1987; Farley et al., 1993). Farley et al. (1993) proposed that the observed variations in helium isotopic compositions might be attributed to the mixing of the plume component, with a heterogeneous distribution of volatiles or having suffered extraction of small degree partial melts prior to mixing, and an asthenospheric component. The Juan Fernandez plume is now thought to sample both FOZO and a relatively depleted component (with MORB-like ^{3}He/^{4}He ratios) during the shield building stage, whereas the rejuvenated phase of the plume sampled mostly the FOZO component (Truong et al., 2018). These two stages, shield and rejuvenated volcanism in the Juan Fernandez Islands, have contrasting patterns of magma ascent and storage (Reyes et al., 2017) and correspond to a classical example of intraplate magmatism fed by a mantle plume; mechanisms also proposed for other OIB, like Hawaii or Réunion. Conversely, Natland (2003) suggested that the helium contents measured in olivine crystals in Juan Fernandez lavas were indicative of mantle-derived volatiles, not derived from a plume, that pervaded magma conduits and storage reservoirs at shallow levels to be trapped in crystallizing olivine.

Highly siderophile elements (HSE: Os, Ir, Ru, Rh, Pt, Pd, Re and Au) and Os isotopes are potential arbitrators for understanding shallow versus deep mantle processes. In basaltic magmas, the HSE show highly compatible (Os, Ir, Ru), to compatible (Pt and Pd) or moderately incompatible (Re) behavior. These elements typically have parallel liquid lines of descent during fractional crystallization, which are controlled by spinel, olivine or sulfide fractionation (e.g. Puchtel and Humayun, 2001; Ireland et al., 2009; Day, 2013). In particular, the partition coefficient for Ru between spinel and melt is one to two orders of magnitude higher than for the other HSE (e.g. Day, 2013). Therefore, HSE signatures in OIB can be dominated by mantle components, due to the corresponding low abundances of these elements in crustal rocks, but can also record shallow level fractionation processes (Day, 2013). This behavior contrasts with other lithophile isotopic systems (Sr-Nd-Pb-Hf) usually documented in OIB; these elements tend to be enriched in crustal and sedimentary rocks (≫ppm level), which can be assimilated by melts and obscure the isotopic and elemental signature of the mantle source (<ppm level).

The long-lived ^{187}Re-^{187}Os decay system (^{187}Re → ^{187}Os + β$^-$; λ = 1.6668 × 10^{-11} a^{-1}; Selby et al., 2007) is an important tool for characterizing the geochemical history of mantle reservoirs. Rhenium and Os have contrasting incompatibilities during melting, with Os being retained within the residue and Re being incompatible, resulting in large isotopic variations generated in crustal reservoirs (^{187}Os/^{188}Os ≥ 1; e.g. Day, 2013 and references

therein), and smaller, generally subchondritic ^{187}Os/^{188}Os variations (^{187}Os/^{188}Os = 0.13) in peridotites (e.g. Day, 2013 and references therein). Abundances of the HSE, coupled with the long-lived ^{187}Re-^{187}Os decay system, are therefore important tools for characterizing the geochemical history of mantle reservoirs and shallow petrogenetic processes affecting magmas and their volcanic products (e.g. Rehkämper et al., 1997; Brandon & Walker, 2005; Day, 2013).

We present whole-rock and olivine separate Os isotope compositions and major- (for olivine separates), trace- and highly siderophile-element abundances for "shield stage" alkali basalts and "post-shield stage or rejuvenated" basanites from the two main islands of the Juan Fernandez Archipelago, Robinson Crusoe and Alexander Selkirk that were previously analyzed by Farley et al. (1993) and Truong et al. (2018) (see Table S1 for the compilation of all data available for the Juan Fernandez lavas and olivine grains), as well as in situ major and highly siderophile-element compositions of the spinel inclusions identified in the olivine grains. The objectives of this study are: (1) to complement the global OIB dataset with lavas from the Juan Fernandez Islands for HSE abundances and Os isotope compositions and compare them with other primitive plume-derived lavas from Hawaii, Réunion or Canary Islands, and (2) investigate the origin of the Juan Fernandez Islands, and in particular the differences in mantle source signature for the lava series from Robinson Crusoe and Alexander Selkirk. Combining Os and He isotopes has the potential to better explain the source contributions in Juan Fernandez lavas, and the origin of their variable ^{3}He/^{4}He ratios.

2. SAMPLES AND METHODS

The samples examined in this study were collected in 1988, during Leg I of the Scripps Institution of Oceanography Hydros expedition. We analyzed 17 basalts (11 samples from Robinson Crusoe; 6 samples from Alexander Selkirk), as well as olivine separates from three of these samples (two from Robinson Crusoe; one from Alexander Selkirk), for their Os isotope compositions, highly siderophile element (HSE: Re, Pd, Pt, Ru, Ir, Os) and trace element abundances. Samples from Robinson Crusoe include 'main shield' olivine tholeiites and alkali basalts, previously termed Group I lavas by Farley et al. (1993), and younger basanite lavas (termed Group II by Farley et al., 1993) that correspond to the rejuvenated post-shield stages of Robinson Crusoe Island (Reyes et al., 2017; Truong et al., 2018). Samples from Alexander Selkirk comprise mostly olivine tholeiites (termed Group III by Farley et al., 1993), and correspond to the main shield stage during formation of the island (Reyes et al., 2017; Truong et al., 2018).

Whole-rock powders and olivine separates were obtained from the study of Truong et al. (2018). The olivine separates were 100% pure olivine, however, dark inclusions were observed in virtually all olivine grains and could not be removed from the separate due to the requirement for sufficient analyte for Os isotope and HSE abundance analyses. Osmium isotope and HSE abundance analyses were

performed at the Scripps Isotope Geochemistry Laboratory (SIGL). One gram of finely ground and homogenized sample powder was precisely weighed and then digested in sealed 20 cm long borosilicate Carius tubes using a mixture of multiply Teflon distilled HCl (4 mL) and 'purged' HNO_3 (7 mL; expunged of Os using H_2O_2), with isotopically enriched multi-element spikes (^{99}Ru, ^{106}Pd, ^{185}Re, ^{190}Os, ^{191}Ir, ^{194}Pt). Digestions lasted for 72 hours in an oven at a maximum temperature of 240 °C.

After digestion, Os was extracted from aqua regia in three steps using CCl_4 and then back-extracted using HBr (Cohen and Waters, 1996), before being purified by micro-distillation (Birck et al., 1997). The other HSE (Re, Pd, Pt, Ru, Ir) were recovered and purified from the residual solutions using anion exchange column chemistry (Day et al., 2014, 2016). Osmium isotopic measurements were performed using a *Thermo Scientific Triton* thermal ionization mass spectrometer in negative ion mode, and Re, Pd, Pt, Ru and Ir abundances were measured using a *Thermo Scientific* iCaP Qc ICP-MS coupled to a *Cetac Aridus II* desolvating nebulizer. Osmium isotope and abundance data were appropriately oxide-, fractionation-, spike- and blank corrected (Day et al., 2016). Precision for $^{187}Os/^{188}Os$, determined by repeated measurements of the 35 pg UMCP Johnson-Matthey standard, was better than ±0.2% (2SD; 0.11357 ± 23; n = 7). Rhenium, Pd, Pt, Ir and Ru isotopic ratios were corrected for mass fractionation using the deviation of standards measured during the run over the natural ratio of the element (Table S2). External reproducibility on HSE analyses was better than 0.9% for 0.5 ppb solutions and all reported values are blank corrected. Total procedural blanks run with samples had $^{187}Os/^{188}Os = 0.22 ± 0.09$ (n = 4; 1 s.d.), with quantities (in pg) of 0.5 ± 0.6 [Re], 11.9 ± 10.5 [Pd], 1.3 ± 0.7 [Pt], 10.2 ± 8.5 [Ru], 1.6 ± 1.3 [Ir] and 2.9 ± 1.1 [Os] (n = 3; 1 s.d.) (see Table S3 for details). Repeat measurements of BHVO-2 and OKUM-1 standards gave $^{187}Os/^{188}Os$ ratios of 0.15317 ± 0.02522 (n = 3) and 0.26471 ± 0.02373 (n = 3) respectively. HSE abundances are (in ng) 0.7 ± 0.02 [Re], 3.2 ± 0.3 [Pd], 14.2 ± 4.9 [Pt], 0.3 ± 0.02 [Ru], 0.1 ± 0.01 [Ir] and 0.3 ± 0.07 [Os] for BHVO-2 (n = 3; 1 s.d.) and 0.6 ± 0.002 [Re], 12.7 ± 0.8 [Pd], 11.1 ± 0.08 [Pt], 4.7 ± 0.02 [Ru], 1.0 ± 0.06 [Ir] and 1.2 ± 0.2 [Os] for OKUM-1 (n = 3; 1 s.d.). The HSE abundances and $^{187}Os/^{188}Os$ ratios for OKUM-1 are consistent with those reported by Savard et al. (2010), Chen et al. (2016) and Maier et al. (2012, 2017). Information regarding run statistics can be found in Tables S2 and S3.

Major and trace elements analyses were performed on 50 mg of homogenized whole rock powder or powdered olivine, using a *Thermo Scientific* iCaP Qc ICP-MS using the method outlined in Day et al. (2014). Samples were prepared and analyzed with powdered rock standards (BHVO-2, BCR-2 and BIR-1a), to confirm accuracy, with reproducibility on most of trace element abundances better than ±5% (with the exception of Ba, Zr and Mo; see Tables S7 and S8 for more information). We find that our new trace element data are in good agreement and expand the available trace elements measured in previous studies (Baker et al., 1987; Farley et al., 1993; Truong et al.,

2018) using both XRF and ICP-MS methodologies. Trace element abundances are reported in Table S6. Major element analyses were performed for the olivines to complement the whole-rock dataset from Farley et al. (1993). We note that Juan Fernandez olivine separates have high Al_2O_3 and TiO_2 content (0.4–1.2 wt% and 0.08–1.9 wt% respectively) compared to other OIB olivine separates like those from Samoa (Jackson & Shirey, 2011; olivine Al_2O_3 content between 0.04 and 0.07 wt%, TiO_2 content between 0.01 and 0.03 wt%), likely reflecting impurities in the measured separates, including spinel grains. The Robinson Crusoe rejuvenated olivine is enriched in incompatible elements compared to the main shield olivine from the same island (Fig. 3). Moreover, the olivine grains in the three different samples display strong positive anomalies in titanium. This is explained by the abundance of chromian titanomagnetite inclusions in the olivine grains, as described by Natland (2003).

Characterization of the spinel inclusions in the olivine grains was performed using a Field Emission Gun Scanning Electron Microscopy (FEG-SEM) coupled with an EDS detector at the University of California San Diego. Map acquisition was performed using one frame count and a pixel dwell time of 100 µs. Spectra were acquired for 20 s. The major element compositions of the spinel inclusions in the olivine grains are reported in Table S4. In-situ HSE abundance analyses of spinel inclusions and olivine grains were performed at the SIGL using a *Thermo Scientific* iCaP Qc ICP-MS coupled with a *New Wave Research* UP213 Laser Ablation System. Ablation analysis took place in a 3 cm³ ablation cell. The cell was flushed with a He-gas flow mixed with Ar as a carrier at ~1 L·min⁻¹. Signals were acquired in Time Resolved Acquisition, devoting around 15 s for the blank and 30 s for measurement of the analyses. Wash time between each analysis was 120 s. The laser was fired using an energy density of ~3.4 J·cm⁻² at a frequency of 5 Hz. Standardization was performed using iron meteorites Hoba, Filomena and Coahuila as certified reference material, using preferred values reported by Day et al. (2018) for the HSE. Because the spinel inclusions were mostly smaller than the beam size, olivine grain compositions were also measured and proportionally subtracted from the spinel measurements. Even though HSE were detected in some of the olivine grains and their spinel inclusions, results were limited by the detection efficiency of the instrument and the sample size. The HSE abundances in the spinel inclusions and olivine grains are reported in Table S5.

3. RESULTS

3.1. Characterization of inclusions in Juan Fernandez olivine grains

Juan Fernandez olivine grains contain numerous inclusions that are mostly spinels (Fig. 2 and Table S4), as previously described by Natland (2003). Spinel inclusions in Robinson Crusoe and Alexander Selkirk main shield olivine grains have higher Cr# (55 ± 7; Cr/[Cr + Al] AFU) and lower Mg# (43 ± 4; Mg/[Mg + Fe] AFU; n = 16) than
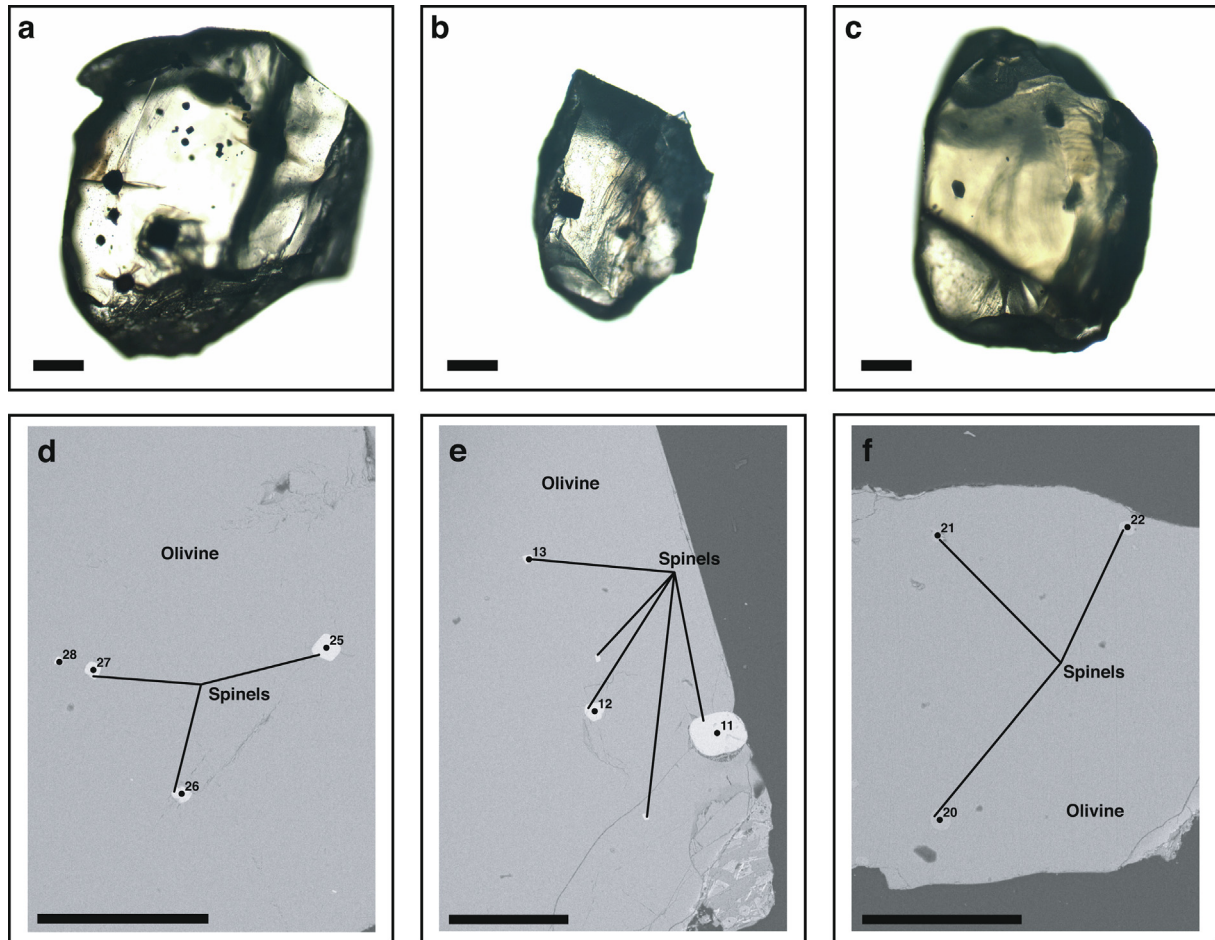
Fig. 2. Spinel inclusions in Juan Fernandez olivine grains. (a) PF-5 (Robinson Crusoe main shield lavas), (b) PF-16 (Robinson Crusoe rejuvenated lavas), (c) MF-3 (Alexander Selkirk main shield lavas). Backscattered images of the spinel inclusions in Juan Fernandez olivine grains (d) PF-5 (Robinson Crusoe main shield lavas), (e) PF-16 (Robinson Crusoe rejuvenated lavas), (f) MF-3 (Alexander Selkirk main shield lavas). The scale bar corresponds to 200 μm.

spinel grains in the rejuvenated lava (Cr# = 12 ± 6; Mg# = 66 ± 2; $n = 4$). Abundances of the HSE for olivine and spinel are reported in Table S5. Spinel inclusions have generally elevated abundances of Re (~0.3 × CI chondrite), Ru, Os and Pd (~0.12 × CI chondrite) and low Ir and Pt compared to their olivine host.

3.2. Trace element abundances

Trace element abundance measurements for Juan Fernandez Islands lavas and olivine separates are reported in Table S6 and Figs. 3 and S1. These new data expand upon – and are in excellent agreement with – previously published Juan Fernandez datasets (Baker et al., 1987; Farley et al., 1993; Truong et al., 2018). Juan Fernandez lavas show enrichment relative to primitive mantle in high field strength elements (HFSE) Ti, Ta and Nb, as reported by Truong et al. (2018), which are common features of most OIB (Jackson et al., 2008; Peters and Day, 2014). The majority of Robinson Crusoe and Alexander Selkirk main shield lavas show positive anomalies in Nb, Ta, Zr, and Sr, and slight negative anomalies in Y. Main shield lavas

also have similar rare earth element (REE) patterns with light REE (LREE) enrichments (Fig. 3). In contrast, Robinson Crusoe basanite lavas have higher absolute trace element abundances than those from the main shield stage and higher Nb/Y at a given Zr/Y (Figs. 3 and 4). This characteristic is also observed in the olivine separates (Fig. 3), which also display strong positive anomalies in titanium (see section 2). Olivine separates have low Mo and W abundances (<0.2 and <0.1 ppm, respectively) compared with main shield lavas from Robinson Crusoe (Mo = 0.72 ± 0.09 ppm; W = 0.23 ± 0.09 ppm) and Alexander Selkirk (Mo = 0.84 ± 0.15 ppm; W = 0.44 ± 0.34 ppm), which in turn, have lower abundances of Mo and W than the basanite lavas from Robinson Crusoe (Mo = 2.23 ± 0.18 ppm; W = 0.88 ± 0.13 ppm) (Fig. S2).

3.3. Osmium isotope compositions and highly siderophile element abundances

Rhenium-osmium isotope and HSE (Re, Pd, Pt, Ru, Ir, Os) abundance measurements for Juan Fernandez Islands lavas and olivine separates are reported in Table 1. Ratios
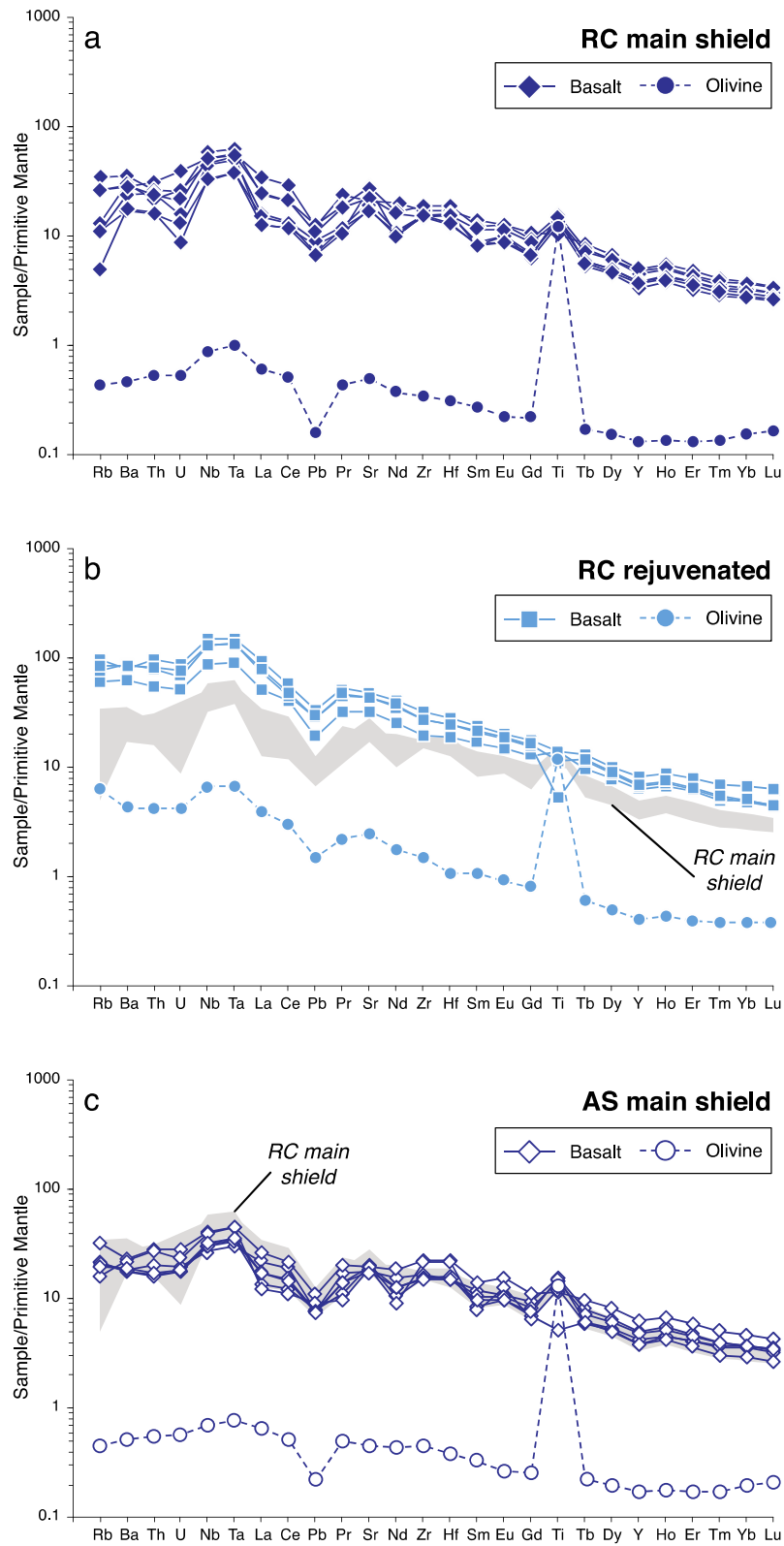
Fig. 3. Primitive mantle normalized multi-element variations diagrams for (a) Robinson Crusoe main shield lavas and olivine, (b) Robinson Crusoe rejuvenated lavas and olivine, and (c) Alexander Selkirk main shield lavas and olivine. Data are normalized to primitive mantle values from McDonough and Sun (1995).
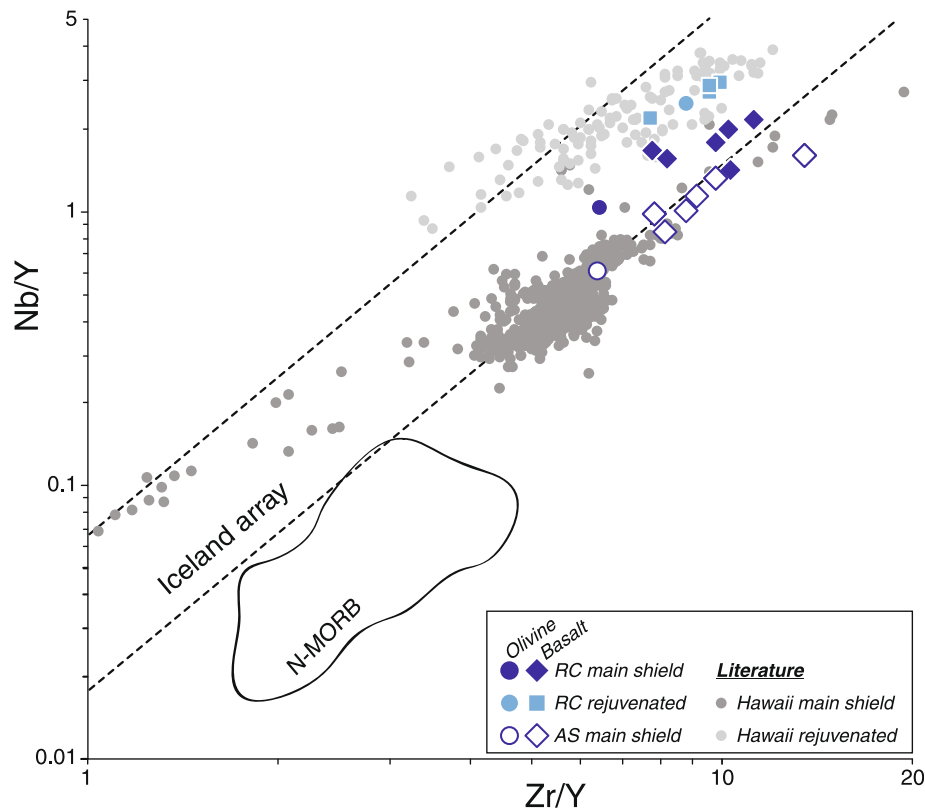
Fig. 4. Niobium/Y versus Zr/Y for Juan Fernandez lavas (diamonds and squares) and olivine grains (circles) compared to Hawaiian rejuvenated (light grey dots) and main shield-stage (dark grey dots) lavas. This diagram discriminates between rejuvenated lavas that form a coherent trend distinct from the main shield lavas (for Juan Fernandez Islands and Hawaii). For the Hawaiian lavas, the offset between these two trends is due to different mantle sources: Hawaiian plume for the main shield lavas and a metasomatized mantle source for the rejuvenated lavas. Various partial melting degrees may also contribute to the vertical offset (e.g. Garcia et al., 2010). RC main shield = Robinson Crusoe main shield lavas and olivine; RC rejuvenated = Robinson Crusoe rejuvenated lavas and olivine; AS main shield = Alexander Selkirk main shield lavas and olivine. Data for Hawaiian main shield stage are from Garcia et al. (1992, 1996, 2000), Mukhopadhyay et al. (2003), Haskins and Garcia (2004), Frey et al. (2016) and references therein, Sinton et al. (2017) and those for the Hawaiian rejuvenated lavas are from Yang et al. (2003), Garcia et al. (2010), Phillips et al. (2016). Diagram after Fitton et al. (1997).

of $^{187}Os/^{188}Os$ were appropriately age-corrected to 4 Ma and 1 Ma, respectively, for the islands of Robinson Crusoe and Alexander Selkirk and we refer to age-corrected values even though age-corrections are negligible (Table 1). Low-Os lavas (10–50 ppt; PV-2, PF-16 Rpt, MF-16, MF-6 Rpt and MF-C4) have variable to radiogenic isotopic compositions (0.1291–0.1435). For samples (including olivine separates) with Os > 50 ppt, $^{187}Os/^{188}Os$ ratios for Robinson Crusoe main shield lavas are 0.1313 ± 0.0022 (Os = 65–910 ppt; 1 s.d., n = 7), with slightly less radiogenic although overlapping values for Alexander Selkirk main shield lavas (0.1291 ± 0.0023; Os = 50–276 ppt; 1 s.d., n = 5) (Fig. 5). The least radiogenic lavas are the basanite samples from Robinson Crusoe (0.1279 ± 0.0046; Os = 180–800 ppt; 1 s.d., n = 4). The osmium isotopic compositions of Juan Fernandez lavas are generally less radiogenic than lavas

from many other ocean islands, and in the range of primitive mantle $^{187}Os/^{188}Os$ (0.1296 ± 0.0008; Meisel et al., 2001).

Olivine separates tend to be less radiogenic than their host lavas ([$^{187}Os/^{188}Os$ Host – $^{187}Os/^{188}Os$ Olivine] × 1000 values range between 3.7 and 6.4), with $^{187}Os/^{188}Os$ ratios between 0.12709 and 0.13032 (0.1283 ± 0.0017), and with Os concentrations between 21 and 138 ppt (Fig. S3). The $^{187}Os/^{188}Os$ composition of the olivine separates are akin to those from Samoa (Jackson and Shirey, 2011) and from Iceland and Jan Mayen (Debaille et al., 2009), which also display high He isotope values.

Robinson Crusoe main shield lavas have relatively flat HSE patterns, approximately ten times lower than Primitive Mantle estimates (Day et al., 2017), with elevated Re contents (Fig. 6a). Alexander Selkirk main shield lavas have

Table 1
Osmium isotope and highly siderophile element abundance data for Juan Fernandez lavas and olivines separates.

Sample	Group[a]	Rock type[b]	Sample type[c]	^{3}He/^{4}He [d]	$\delta^{18}O_{Ol}$ [e]	MgO (wt%)[f]	Re (ppb)	Pd (ppb)	Pt (ppb)	Ru (ppb)	Ir (ppb)	Os (ppb)	^{187}Re/^{188}Os	^{187}Os/^{188}Os [g]	^{187}Os/^{188}Os age corr [i]	2σ
PV-2	I	A.B.	WR	13.6	5.0	8.65	0.543	0.24	0.24	0.24	0.048	0.037	70.7	0.14467	0.14349	0.00181
PV-4	I	O.T.	WR	14.5		19.87	1.069	0.40	0.93	0.54	0.52	0.603	8.43	0.13051	0.13037	0.00014
PF-3	I	A.B.	WR	15.1	5.1	14.72	0.171	0.28	0.35	0.36	0.085	0.187	4.35	0.13410	0.13402	0.00127
PF-5	I	A.B.	WR	15.3	5.0	10.66	0.177	1.08	0.60	0.30	0.21	0.281	2.99	-	-	-
	I	A.B.	Rpt			10.66	0.169	0.93	0.65	0.34	0.11	0.102	7.85	0.13413	0.13400	0.00011
	I	Olivine	Olivine	15.3	5.0	47.30	0.016	0.24	0.16	0.83	0.033	0.065	1.21	0.12764	0.12762	0.00041
PF-10	I	O.T.	WR	15.8		15.74	0.155	-	0.46	0.52	0.16	0.208	3.55	0.13059	0.13053	0.00045
PIN-12	I	O.T.	WR	16.6		19.88	0.127	0.98	0.76	0.44	0.13	0.140	4.30	0.13146	0.13139	0.00058
PIN-8	I	O.T.	WR	17.2	5.0	21.41	0.115	0.65	0.58	0.54	0.27	0.905	0.60	0.13090	0.13089	0.00096
PF-16	II	BSN	WR	11.2		13.61	0.253	0.17	0.081	0.21	0.005	0.078	15.4	-	-	-
	II	BSN	Rpt			13.61	0.246	0.10	0.10	0.26	0.040	0.010	119	0.13632	0.13433	0.00036
	II	Olivine	Olivine	11.2		44.54	0.038	0.13	0.047	0.26	0.023	0.021	8.70	0.13047	0.13032	0.00024
PV-1	II	BSN	WR	12.3	5.3	10.72	0.308	0.47	0.59	0.40	0.12	0.179	8.18	0.13239	0.13225	0.00025
PF-21	II	BSN	WR	12.4		11.99	0.276	0.39	0.78	0.67	0.28	0.800	1.64	0.12174	0.12172	0.00048
PF-17	II	BSN	WR	12.5	5.3	12.63	0.436	0.48	0.72	0.77	0.49	0.590	3.51	0.12738	0.12732	0.00026
MF-C4	III	O.T.	WR	7.8		13.57	0.139	0.16	0.10	0.26	0.043	0.050	13.1	0.13859	0.13772	0.00068
MF-3	III	O.T.	WR	8.0	5.0	8.53	0.058	0.15	0.14	0.24	0.085	0.066	4.15	0.13107	0.13079	0.00079
	III	Olivine	Olivine	8.0		44.07	0.018	0.07	0.06	0.58	0.043	0.138	0.61	0.12713	0.12709	0.00010
MF-16	III	O.T.	WR	8.1		10.49	0.196	2.15	0.51	0.42	1.21	0.046	20.1	0.13046	0.12912	0.00040
MF-6	III	O.T.	WR	8.2		11.38	0.177	-	0.15	0.17	0.075	0.114	7.36	-	-	-
	III	O.T.	Rpt			11.38	0.173	0.13	0.16	0.27	0.010	0.038	21.6	0.12969	0.12825	0.00035
MF-S1	III	A.B.	WR	8.6		19.79	0.092	0.27	123	0.41	0.090	0.118	3.71	0.13250	0.13225	0.00041
	III	A.B.	Rpt			19.79	0.074	0.14	233	0.84	0.22	0.268	1.31	0.12579	0.12570	0.00016
MF-C2	III	O.T.	WR	9.5		14.38	0.073	0.081	0.27	0.19	0.12	0.076	4.59	-	-	-
	III	O.T.	Rpt			14.38	0.056	0.089	0.23	0.33	0.015	0.057	4.68	0.13110	0.13079	0.00024

[a] Grouping classification of Farley et al. (1993) for the lavas. Group I = main shield, Robinson Crusoe; Group II = basanites, Robinson Crusoe; Group III = main shield, Alexander Selkirk.
[b] A.B. = alkali basalt; O.T. = olivine tholeiite; BSN = basanite.
[c] WR: whole rock; Rpt: replicate.
[d] Farley et al. (1993).
[e] Eiler et al. (1997).
[f] olivine (this study), lavas (Baker et al., 1987).
[g] Measured values.
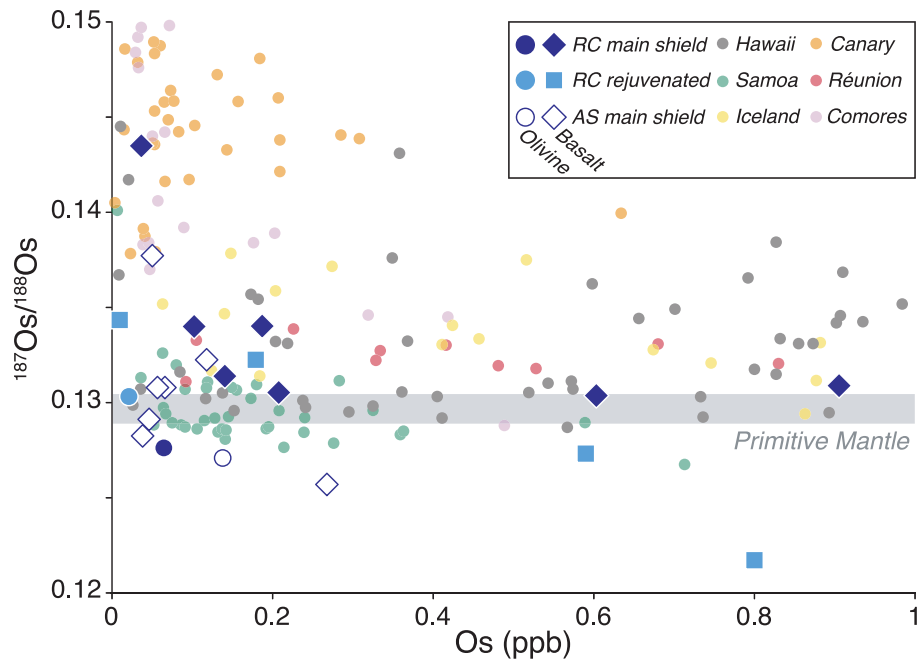[i] Age corrected values: Robinson Crusoe lavas for 4 Ma, Alexander Selkirk lavas for 1 Ma.

Fig. 5. Plot of $^{187}Os/^{188}Os$ ratios versus Os abundances for Juan Fernandez lavas (diamonds and squares) and olivine separates (circles), compared with lavas from Hawaii (Jamais et al., 2008; Ireland et al., 2009), the Comores Islands (Class et al., 2009), Réunion Island (Peters et al., 2016), the Canary Islands (Day et al., 2010), Iceland (Brandon et al., 2007) and Samoa (Jackson & Shirey, 2011). $^{187}Os/^{188}Os$ ratios greater than 0.15 for OIB from Hawaii, Samoa, the Canary Islands and the Comores Islands are not represented. RC main shield = Robinson Crusoe main shield lavas and olivine; RC rejuvenated = Robinson Crusoe rejuvenated lavas and olivine; AS main shield = Alexander Selkirk main shield lavas and olivine. The grey field represents the primitive mantle range for $^{187}Os/^{188}Os$ from Meisel et al. (2001).

generally lower absolute HSE abundances than Robinson Crusoe main shield lavas, with prominent Ru anomalies, and one sample also shows Pd and Ir enrichment (MF-16; Fig. 6c). Sample MF-S1 also has anomalously high concentrations of Pt (>100 ppb); for clarity this datum is not shown in Fig. 6. Robinson Crusoe basanites have a range of HSE abundances spanning those observed in the Robinson Crusoe and Alexander Selkirk main shield lavas (Fig. 6b). Olivine separates tend to have lower HSE abundances compare to their host lava, with the exception of a strong positive Ru anomaly. Absolute HSE abundances of Juan Fernandez lavas are generally lower than for lavas from Hawaii (Ireland et al., 2009), Réunion (Peters et al., 2016) and the Canary Islands (Day et al., 2010), but show similar inter-element HSE variations (Figs. 7 and S4).

4. DISCUSSION

4.1. Rejuvenated and main shield lavas and clarification of prior groupings

Flexural uplift of the lithosphere in response to far-field stresses can lead to rejuvenated volcanism. On mature oceanic plate, such as around Hawaii, uplift of the elastic lithosphere occurs up to 200 km downstream from the active load, leading to decompression of the underlying asthenosphere (e.g., Bianco et al., 2005) and generation of rejuvenated basaltic lavas characterized by depleted isotopic signatures (e.g., Bizimis et al., 2013; Garcia et al., 2016) and higher Nb/Y ratios at a given Zr/Y ratio than for main

shield stage basalts (Fig. 4), suggesting distinct mantle sources for the main shield stage and rejuvenated stage lavas.

Post-erosional lavas from Robinson Crusoe bear many of the hallmarks of rejuvenated lavas (see also, Reyes et al., 2017; Truong et al., 2018). These lavas are low-degree partial melts (basanites; Fig. S5) that are enriched in incompatible elements compared to the main shield lavas from Robinson Crusoe, and also have relatively depleted Sr and Nd isotope signatures (Baker et al., 1987; Farley et al., 1993; Reyes et al., 2017; Truong et al., 2018). As with Hawaii, Robinson Crusoe rejuvenated lavas also have higher Nb/Y ratios at a given Zr/Y than those from the main shield stage. We also find that these rejuvenated lavas span a larger range of HSE abundances and have generally lower and more variable Os isotopes ratios than main shield lavas (Fig. 5). Because there is no correlation between HSE abundances with fractional crystallization indicators like MgO (Fig. S4), these variations likely reflect a greater degree of lithospheric interaction, where the oceanic lithosphere has relatively unradiogenic Os isotopic compositions and high HSE abundances (e.g., Day et al., 2017).

Generation of rejuvenated lavas on Robinson Crusoe at ~0.9 Ma ($^{40}Ar/^{39}Ar$ age reported for one basanite from Santa Clara Island by Reyes et al., 2017) are consistent with loading of the lithosphere by the formation of Alexander Selkirk (between 0.83 and 0.94 Ma) some 180 km away at a plate velocity of 74 mm.yr^{-1} (DeMets et al., 2010). Since the Robinson Crusoe basanites can be classified as rejuvenated lavas, we clarify that the previous compositional grouping scheme of Farley et al. (1993) for the basalts
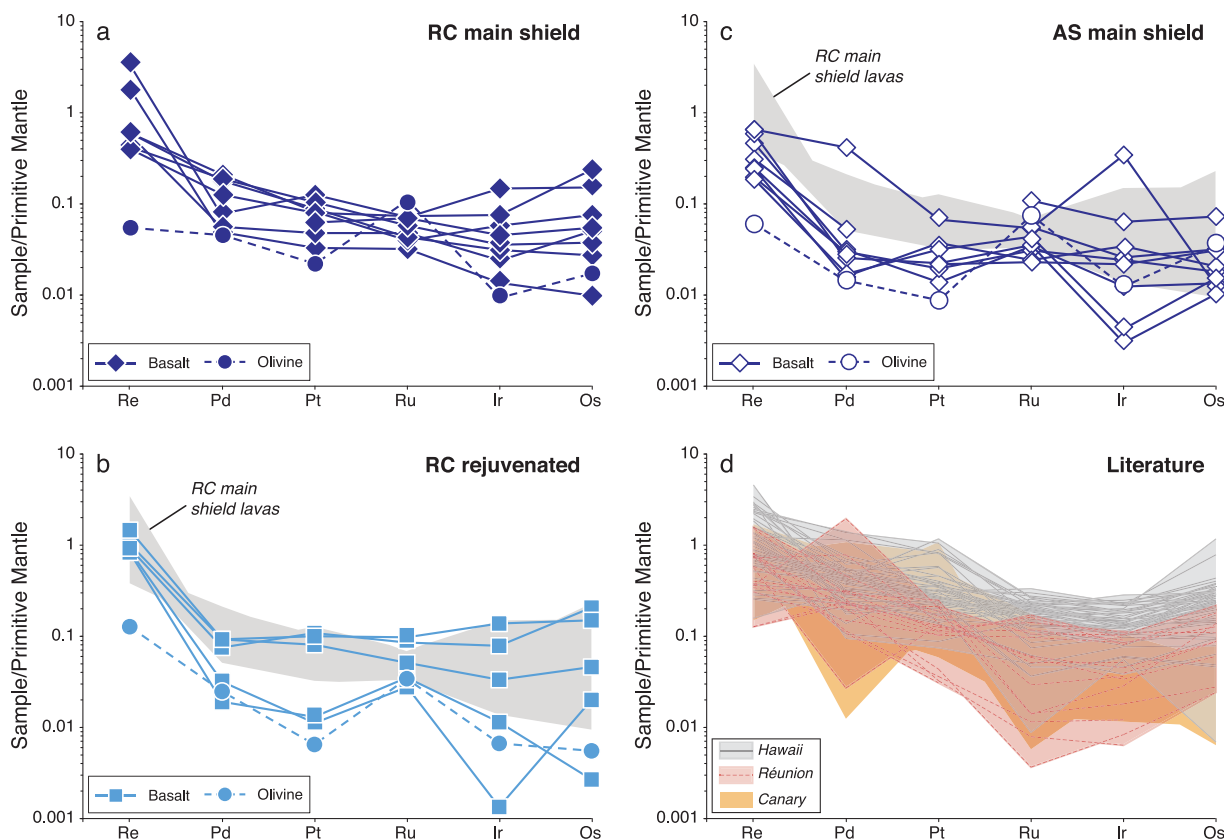
Fig. 6. Highly siderophile element patterns for Juan Fernandez lavas (diamonds or squares and straight lines) and olivine separates (circles and dashed lines). (a) Robinson Crusoe main shield lavas and olivine; (b) Robinson Crusoe rejuvenated lavas and olivine; (c) Alexander Selkirk main shield lavas and olivine; (d) comparison of lavas from Hawaii (Ireland et al., 2009), the Canary Islands (Day et al., 2010) and Réunion Island (Peters et al., 2016). Data are normalized relative to Primitive Mantle (PM) values from Day et al. (2017).

Fig. 7. Ruthenium abundances as a function of MgO content for Juan Fernandez lavas (diamonds and squares; olivine grains are not shown), compared with lavas from Hawaii (Ireland et al., 2009), Réunion Island (Peters et al., 2016) and the Canary Islands (Day et al., 2010). RC main shield = Robinson Crusoe main shield lavas; RC rejuvenated = Robinson Crusoe rejuvenated lavas; AS main shield = Alexander Selkirk main shield lavas.

(Group I = Robinson Crusoe main shield; Group II = Robinson Crusoe basanites; Group III = Alexander Selkirk main shield) is consistent with the distinct volcanism mechanisms for their formation.

4.2. Crystal-liquid fractionation defines Juan Fernandez lava HSE compositions

During ascent through the oceanic crust towards the surface, mantle-derived magmas can assimilate significant volumes of crustal material, which can alter the HSE abundances and Os isotopic composition of the melt (e.g. Roy-Barman and Allègre, 1995; Lassiter and Hauri, 1998; Widom et al., 1999; Day et al., 2010). As Os is more compatible than Re during partial melting, large isotopic variations between mantle-derived materials ($^{187}Os/^{188}Os < 0.18$) and crustal or sedimentary materials occur with time ($^{187}Os/^{188}Os \geq 0.4$; Day, 2013). OIB with Os contents lower than 50 ppt are considered to be more susceptible to contamination by high $^{187}Os/^{188}Os$ crustal materials (e.g. Day, 2013). A few samples among Juan Fernandez lavas have low Os concentrations (≤ 50 ppt), associated with radiogenic Os isotope compositions for two samples (MF-C4 = 0.13772 and PV-2 = 0.14349). Aside from these samples, assimilation processes play a limited role in Juan Fernandez main shield lava HSE compositions.

To quantify the role of fractional crystallization in the HSE fractionation for Juan Fernandez lavas, we used a model assuming olivine-melt and spinel-melt control using a calculated parental melt composition. The parent melt composition was obtained using a log-log variation diagram of Al_2O_3 versus MgO which allows discrimination between samples that witnessed olivine and clinopyroxene accumulation or removal by a break in slope at ~11 to 12 wt% Al_2O_3 and ~14 to 16 wt% MgO. The parent melt composition was then derived from linear regressions of HSE versus MgO trends at 15 ± 1 wt%. These calculations indicate that the parental melts of lavas from Robinson Crusoe and Alexander Selkirk have broadly similar HSE contents. The amounts of early-formed spinel and olivine crystallization permissible for Juan Fernandez lavas were calculated with Petrolog (Danyushevsky and Plechov, 2011) for fractional crystallization of olivine and spinel at a range of pressures (1, 2, 5 and 10 kbar). Starting compositions were chosen as closest to the parent melt composition (MgO = 15 wt%) for each of the three groups of lavas (PF-10, PF-16 and MF-C2 for Robinson Crusoe main shield lavas, Robinson Crusoe rejuvenated lavas and Alexander Selkirk main shield lavas respectively). Major element compositions for Juan Fernandez main shield lavas (e.g. Al_2O_3 or CaO contents in function of MgO) can be explained by up to 30% of olivine fractionation (together with spinel crystallization of up to 5%) between 1 and 5 kbar. On the other hand, Robinson Crusoe rejuvenated lavas compositions can be reproduced at higher-pressure fractional crystallization (up to 10 kbar): these mantle-derived melts experienced rapid ascent to the surface with a deeper crystallization history. These results are consistent with Baker et al. (1987) and Reyes et al. (2017) who suggested shallow storage conditions for the shield stage lavas (~1–3 kbar) and rapid ascent with polybaric crystallization for the basanitic lavas (starting ~10 kbar).

Fractionation of olivine (up to 30%) alone from estimated parental melts produces residual melts with HSE abundances similar to the observed compositions for Juan Fernandez Islands but does not explain the shape of the observed HSE patterns for the olivines, with a positive anomaly in Ru (ol/melt partition coefficients from Puchtel and Humayun, 2001). Ruthenium, Ir and Os are similarly compatible in olivine but Ru is highly compatible in spinel compared to the other HSE, and in particular to Ir and Os (e.g. Brenan et al., 2012). A notable feature of the Juan Fernandez olivine separates that we measured is a strong positive Ru anomaly (Fig. 6). This can be explained by spinel crystallization and, then, inclusion in the olivine grains (Fig. 2), further suggesting fractionation of both early-formed spinel and olivine. The method used to estimate the parent melt composition is associated with large uncertainties for HSE abundance estimates, which could explain why we are not able to reproduce the compositional range shown in Fig. 8a. The incorporation of early-formed spinel (up to 5%) to the olivine grains can explain the generation of anomalously high Ru contents in olivine, due to the high compatibility of Ru in spinel (partition coefficients for sp/melt from Righter et al., (2004) for Re and Brenan et al. (2012) for Pd, Pt, Ir, Ru (see compilation in Day, 2013)).

Fractionation of up to 30% of olivine (ol/melt partition coefficients for REE from Fujimaki et al., 1984) from a starting composition closest to the parent melt composition for each of the three groups of the Juan Fernandez lavas produces REE patterns similar to those of the Juan Fernandez olivines for the HREE but that are too depleted for the LREE. The addition of 1–5% spinel (sp/melt partition coefficients for REE from Nagasawa et al., 1980) is also insufficient to reproduce the REE patterns we observe for Juan Fernandez olivine grains. However, the contamination by a small fraction (1–2% for the main shield lavas from both islands, up to 5% for the rejuvenated lavas) of the host lava
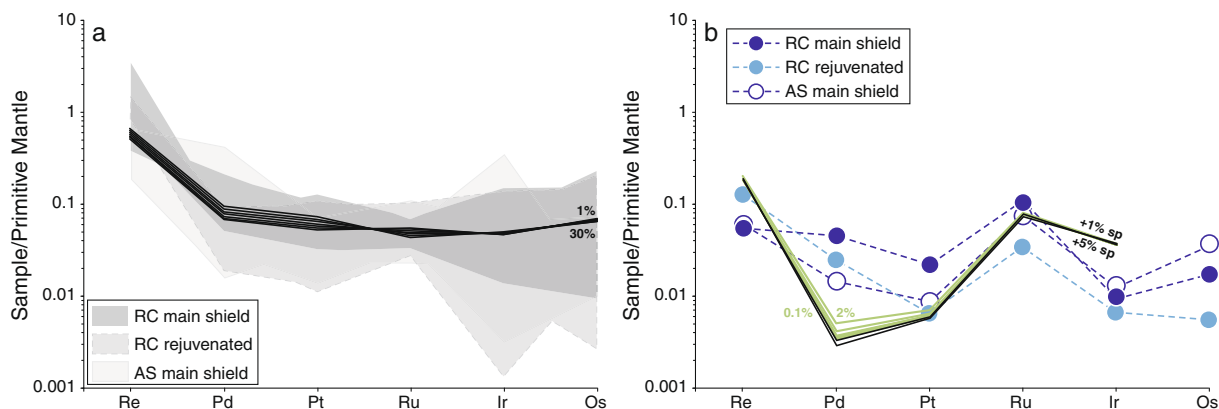

Fig. 8. (a) Modeled compositions of residual melts after fractional crystallization of 1%, 5%, 10%, 15%, 20%, 25% and 30% of olivine (black lines) compared with the compositional ranges of Juan Fernandez lavas (Robinson Crusoe main shield basalts, Robinson Crusoe rejuvenated lavas, and Alexander Selkirk main shield basalts). (b) Composition of olivine after 30% of fractional crystallization from the parent melt of Juan Fernandez lavas, with various amounts of spinel (1% and 5%; black lines) to reproduce the contribution of the spinel inclusions to the HSE composition of olivine separates. The green lines correspond to the composition of the previous mixture of olivine with +5% spinel to which we added the contribution of 0.1–2% of the average HSE composition of Juan Fernandez basalts (see Fig. 9 for the fractional crystallization modeling of the REE). The parent melt composition was derived from linear regressions of HSE versus MgO trends (see text). The fractionation of 1–5% of spinel from the parental melt does not significantly affect the composition of the melt. Partition coefficients for ol/melt and sp/melt are given in the text. Data are normalized relative to Primitive Mantle (PM) values from Day et al. (2017).

(melt) is sufficient to enrich the olivine in LREE to the observed abundances, implying that silicate melt inclusions are also present in some olivine grains (Fig. 9), which is consistent with petrographic observations (Natland, 2003). Contamination by the melt inclusions of the HSE signature of the olivine grains tends to lower the negative Pd anomaly of the calculated composition, although overall, it has a limited effect on the HSE signature of the olivine separates (Fig. 8).

4.3. Comparison of OIB main shield and rejuvenated lavas

The Alexander Selkirk main shield lavas are lithologically and compositionally similar in terms of major and trace element abundances to Robinson Crusoe main shield basalts (Baker et al., 1987; Farley et al., 1993), whereas the Robinson Crusoe basanite lavas (rejuvenated lavas) have higher abundances of incompatible trace elements, interpreted as resulting from lower degrees of partial melting than for the main shield stage (Baker et al., 1987; Farley et al., 1993; Reyes et al., 2017 and Fig. S5). Samples from these three groups exhibit a large range in ^{3}He/^{4}He ratios (7.8–18.0 R_A): Robinson Crusoe shield basalts have ^{3}He/^{4}He ratios between 13.6 and 18.0 R_A, whereas Robinson Crusoe post-shield basanites range from 11.2 to 12.9 R_A (Farley et al., 1993; Truong et al., 2018). Main shield basalts from Alexander Selkirk show lower and more uniform ^{3}He/^{4}He ratios with an average value of 8.3 ± 0.5 R_A (Farley et al., 1993). Previous studies have shown limited variations for ^{87}Sr/^{86}Sr (0.70340–0.70378) and ^{143}Nd/^{144}Nd ratios (0.512835–0.512918) (Gerlach et al., 1986; Baker et al., 1987; Farley et al., 1993; Truong et al., 2018). On average, Robison Crusoe main shield basalts are the most isotopically heterogeneous in terms of Sr and Nd isotopic compositions, while the rejuvenated basanites lie at the most depleted end of the trend defined by

Robinson Crusoe main shield basalts (lower ^{87}Sr/^{86}Sr and higher ^{143}Nd/^{144}Nd). Main shield basalts from Alexander Selkirk show homogeneous compositions, with higher ^{143}Nd/^{144}Nd at a given ^{87}Sr/^{86}Sr than those from Robinson Crusoe. Robinson Crusoe basalts and basanites have slightly more radiogenic ^{206}Pb/^{204}Pb ratios (19.163–19.292) than Alexander Selkirk basalts (18.939–19.221) (Truong et al., 2018). Overall, Sr-Nd-Pb isotopic compositions suggest that all the samples are from a common, albeit slightly heterogeneous mantle source (Gerlach et al., 1986; Baker et al., 1987; Farley et al., 1993; Truong et al., 2018).

Alexander Selkirk main shield lavas have been dated between 0.83–0.94 Ma (Lara et al., 2018b), ca. 2–3 Ma younger than Robinson Crusoe main shield lavas. A ^{40}Ar/^{39}Ar age of 0.9 ± 0.03 Ma has also been reported by Reyes et al. (2017) for a basanite from Santa Clara Island. Even though no radiometric ages are available for Robinson Crusoe rejuvenated lavas, they are clearly younger as they intruded or cross-cut the main shield lavas (Reyes et al., 2017). They are most likely to be contemporaneous with the creation of Alexander Selkirk Island. Robinson Crusoe rejuvenated basanites have slightly less radiogenic and more variable ^{187}Os/^{188}Os ratios than Alexander Selkirk main shield lavas, associated with higher ^{3}He/^{4}He values (11.2–12.9 R_A for Robinson Crusoe rejuvenated lavas, and 7.8–9.5 R_A for Alexander Selkirk main shield lavas).

Konter and Jackson (2012) reported ^{187}Os/^{188}Os ratios for Samoan rejuvenated lavas that are similar to ^{187}Os/^{188}Os ratios for Samoan peridotite xenoliths (Jackson et al., 2016), and exhibit lower ^{187}Os/^{188}Os values than those for the Samoan main shield lavas (Fig. 10). The Samoan xenoliths most likely originate from within the mantle lithosphere (Hauri and Hart, 1994), such that the Os isotope values in Samoan rejuvenated lavas are derived from the lithospheric mantle, suggesting melting during Samoan rejuvenation stage occurs close to the
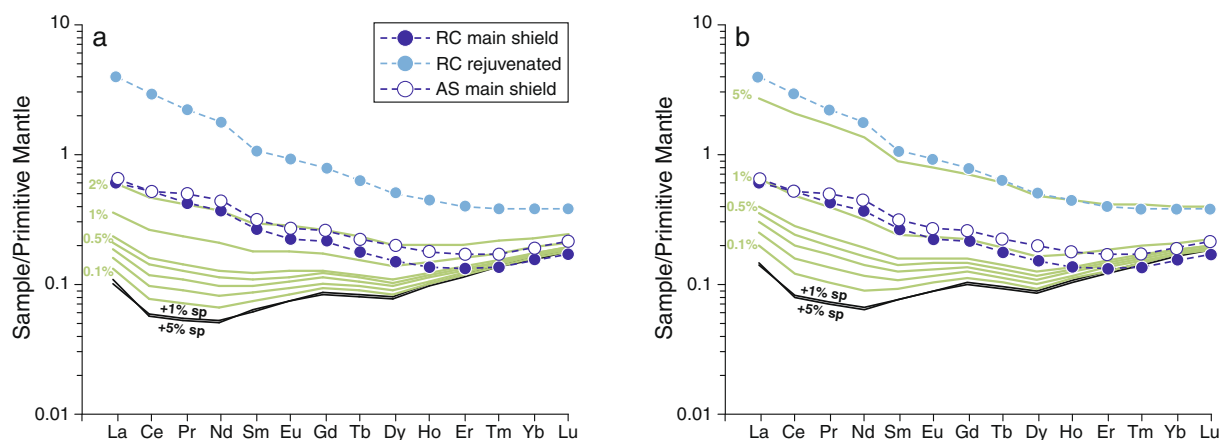

Fig. 9. Composition of olivine after 30% of fractional crystallization from the parent melt of Juan Fernandez lavas, mixed with various amounts of spinel (1% and 5%; black lines) to reproduce the contribution of spinel inclusions to the olivine REE composition. The green lines correspond to the composition of the previous assemblage olivine +5% spinel, to which we added the contribution of 0.1–5% of the composition of the starting material: (a) main shield lava composition, (b) rejuvenated lava composition. Juan Fernandez olivine separates are shown for comparison. As the starting melt composition, we used PF-10 and PF-16, which are the closest to the parent melt composition in terms of MgO content, for Robinson Crusoe main shield and rejuvenated lavas respectively. Partition coefficients for ol/melt are from from Fujimaki et al. (1984), and those for sp/melt from Nagasawa et al. (1980). Data are normalized relative to Primitive Mantle (PM) values from McDonough & Sun (1995).
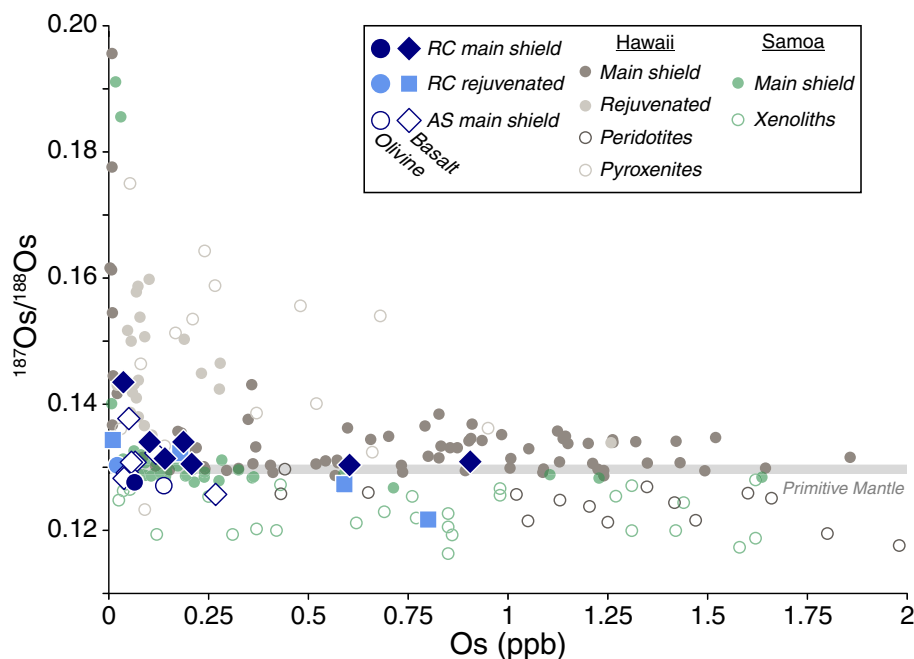
Fig. 10. Plot of ^{187}Os/^{188}Os ratios versus Os abundances for Juan Fernandez lavas (diamonds and squares) and olivine separates (circles), compared with main shield lavas (Hawaii: Jamais et al., 2008; Ireland et al., 2009; Samoa: Jackson & Shirey, 2011), rejuvenated lavas (Hawaii: Lassiter et al., 2000; Samoa: Konter and Jackson, 2012), xenoliths (Hawaii: peridotites from Lassiter et al., 2000: Bizimis et al., 2007; pyroxenites from Lassiter et al., 2000; Sen et al., 2011; Samoa: Jackson et al., 2016). RC main shield = Robinson Crusoe main shield lavas and olivine; RC rejuvenated = Robinson Crusoe rejuvenated lavas and olivine; AS main shield = Alexander Selkirk main shield lavas and olivine. The grey field represents the primitive mantle range for ^{187}Os/^{188}Os from Meisel et al. (2001).

lithosphere-asthenosphere boundary (Konter and Jackson, 2012). Additionally, Samoan rejuvenated lavas have lower in ^{206}Pb/^{204}Pb and ^{208}Pb/^{204}Pb, and intermediate in ^{87}Sr/^{86}Sr and ^{143}Nd/^{144}Nd compared to the shield lavas (Fig. S6 and Konter and Jackson, 2012). These later observations are also consistent with sampling of a lithospheric component (Konter and Jackson, 2012). Hawaiian rejuvenated lavas, on the other hand, have highly variable Os isotope compositions than range to more radiogenic values than the main shield lavas, similar to pyroxenite xenoliths (Fig. 10), whereas peridotite xenoliths have subchondritic Os ratios (Lassiter et al., 2000; Bizimis et al., 2007; Sen et al., 2011). Hawaiian rejuvenated lavas also have more depleted Sr- (and Nd-) isotope compositions than the main shield lavas (Fig. S6). Lassiter et al. (2000) proposed that moderate-degree pyroxenite partial melts in the source of the rejuvenated lavas are most likely the source of the radiogenic Os isotope signature due to correlations between Os isotopes and both major and trace element abundances in the rejuvenated lavas. These results indicate strong similarities in rejuvenated lavas from Juan Fernandez, Samoa and Hawaii.

The Robinson Crusoe basanites also exhibit depleted Sr and Nd isotopes signatures (Baker et al., 1987; Farley et al., 1993; Reyes et al. 2017; Truong et al., 2018) compared to Robinson Crusoe main shield lavas, and have lower ^{143}Nd/^{144}Nd at a given ^{87}Sr/^{86}Sr than Alexander Selkirk main shield lavas. No distinction is observed between the three types of lavas in terms of ^{207}Pb/^{204}Pb. However, Alexander Selkirk main shield lavas are less radiogenic in Pb isotopes

than Robinson Crusoe main shield and rejuvenated lavas, which have overlapping ^{206}Pb/^{204}Pb and ^{208}Pb/^{204}Pb. Thus, the relative sense of isotopic variability in Juan Fernandez main shield and rejuvenated lavas is similar to those in Samoan and Hawaiian main shield and rejuvenated lavas (Garcia et al., 2010; Konter and Jackson, 2012), and are consistent with a lithospheric source for rejuvenated lavas (Bianco et al., 2005; Konter and Jackson 2012).

As noted above, Robinson Crusoe rejuvenated lavas have higher ^{3}He/^{4}He values than Alexander Selkirk main shield lavas and lower than Robinson Crusoe main shield lavas. We propose that the lithosphere was polluted by noble gases from the main shield building phase of Robinson Crusoe Island during the ascent of the melts through the lithosphere. These noble gases then contaminated Robinson Crusoe rejuvenated melts explaining their elevated ^{3}He/^{4}He signatures. Model mixtures of a MORB-like depleted component (D) and a high-^{3}He hotspot endmember (P) are presented in Fig. 11 and show that Robinson Crusoe rejuvenated lavas lie between the main shield lavas from Robinson Crusoe and Alexander Selkirk (curves B and C), and correspond to 40–60% of contamination of the depleted mantle component by a degassed plume component (curves B and C), corresponding to an open-system where the plume component would have been degassed of its mantle-derived He. This is similar to the mixing model proposed by Farley et al. (1993) between two endmembers Primitive Helium Mantle (PHEM) and the depleted MORB mantle (DMM) to reproduce Juan Fernandez lavas compositions.
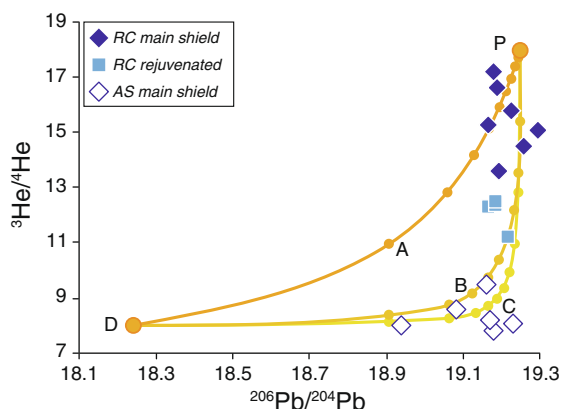
Fig. 11. Plot of He versus Pb isotope variation for Juan Fernandez samples illustrating binary mixing trajectories between a depleted component (D) and a high-³He hotspot endmember (P). Isotopic values for D are from Hilton et al. (2000). The He isotope characteristics of P is taken as 18 R_A, as the highest ratio measured for Robinson Crusoe main shield lavas (Farley et al., 1993). The plume lead isotopic composition ²⁰⁶Pb/²⁰⁴Pb is taken as 19.25 in order to be slightly higher than the average isotopic composition for Robinson Crusoe main shield lavas. Curves are labeled to represent the mixing with variably degassed plume sources: (A) undegassed mantle plume ⁴He abundance is taken as 56 μcm³STP/g, which is the ⁴He content in PIN-8 and the value for the undegassed mantle used by Hilton et al., 2000), (B) and (C) represent depletions of x12 and x36, respectively, relative to the initial plume He content. Dots along the mixing curves represent a 10% increment in the mixing proportions between the two endmembers. RC main shield = Robinson Crusoe main shield lavas; RC rejuvenated = Robinson Crusoe rejuvenated lavas; AS main shield = Alexander Selkirk main shield lavas.

4.4. Implications for high-³He/⁴He and heterogeneous mantle plumes

Amongst OIB, Juan Fernandez lavas span an unusual isotopic compositional range: Juan Fernandez lavas overlap with Samoan lavas that are close to FOZO or C in terms of ¹⁸⁷Os/¹⁸⁸Os, ²⁰⁶Pb/²⁰⁴Pb, ²⁰⁸Pb/²⁰⁴Pb and ¹⁴³Nd/¹⁴⁴Nd ratios, but have lower ³He/⁴He ratios, intermediate between high-³He/⁴He OIB (like Samoan, Icelandic and Hawaiian lavas) and low-³He/⁴He OIB (Canary Islands and the Comores) (Fig. 12). Overall, Juan Fernandez lavas converge at FOZO or C of the global OIB dataset (e.g. Hart et al., 1992; Hanan and Graham, 1996; Day et al., 2010; Truong et al., 2018). Juan Fernandez Islands display isotopic characteristics of a considerable range in ³He/⁴He (7.8–18 R_A), but limited variability in Sr, Nd, Pb and Os isotopic ratios. Whereas HSE and trace element abundances are controlled by melting and fractional crystallization, isotopic compositions of the Juan Fernandez lavas seem unaffected by fractional crystallization and assimilation processes. In particular, fractional crystallization and other petrogenetic processes cannot account for the high ³He/⁴He in Juan Fernandez lavas, as no correlation is observed between ³He/⁴He ratios and fractionation indicators like MgO. Thus, it seems that ³He/⁴He and bulk He of Juan Fernandez lavas are derived from the mantle plume and the differentiation processes experienced by the parent melts derived from this source, and not from volatiles that permeated shallow magma reservoirs (c.f. Natland, 2003).

Mantle plume sources can vary significantly in ³He/⁴He temporally and spatially, such as Samoa (19.5–33.8 R_A – Jackson et al., 2007), Hawaii (6–28 R_A – Mukhopadhyay et al., 2003; up to 29.3 R_A – Valbracht et al., 1997)) and Iceland (9.6–19 R_A – Brandon et al., 2007; up to 37.7 R_A – Hilton et al., 1999; and even 47.5 R_A – Harðardóttir et al., 2018). Variations in ³He/⁴He ratios are also observed for Juan Fernandez Islands: starting with inception of high ³He/⁴He (Robinson Crusoe main shield lavas) that also impregnates the lithosphere with ³He (Robinson Crusoe rejuvenated lavas) followed by lower ³He/⁴He in Alexander Selkirk. Robinson Crusoe and Alexander Selkirk main shield lavas, however, are distinct in terms of radiogenic (Sr-Nd-Pb-Os) and noble gas (He) isotope compositions. Within the Juan Fernandez Islands, Robinson Crusoe main shield lavas are the most enriched samples with lower ¹⁴³Nd/¹⁴⁴Nd and higher ²⁰⁶Pb/²⁰⁴Pb, ²⁰⁸Pb/²⁰⁴Pb, ¹⁸⁷Os/¹⁸⁸Os and ³He/⁴He compared to Alexander Selkirk main shield lavas. The distinction between Robinson Crusoe and Alexander Selkirk main shield lavas suggests an isotopic zonation in the mantle plume.

Huang et al. (2011) showed that geochemical zoning might be a common feature of mantle plumes beneath the Pacific plate: two subparallel arrays of volcanoes exist at Hawaii, Samoa, and the Marquesas, with the southern trend of volcanoes being more radiogenic in lead and less radiogenic in neodymium. Huang et al. (2011) proposed that isotopically enriched material is preferentially distributed in the lower mantle of the Southern Hemisphere, within the Pacific low seismic velocity zone. The distribution of heterogeneity in the Thermal Boundary Layer would result in bilaterally zoned plume conduits at Hawaii and the Marquesas, Samoa being more complex. A bilaterally zoned plume model has previously been proposed for the Hawaiian plume (Abouchami et al., 2005). Weis et al. (2011) proposed that the geochemical differences between the Kea and Loa trends reflect preferential sampling of two distinct sources of deep mantle material: the Loa trend sampling LLSVP (Large Low-Shear Velocity Province) material, and the Kea trend sampling lower mantle material. Alternatively, Farnetani & Hofmann (2009, 2010) have proposed that a continuous deep layer overlained by a bilaterally varying layer best reproduces the "bilateral asymmetry" observed for Pb isotopic differences between the Kea and Loa-trends of Hawaiian volcanoes and for the concentric distribution of ³He/⁴He (DePaolo et al., 2001). It has also been suggested that high-³He/⁴He materials could be distributed as isolated primitive blobs in the lower mantle (Becker et al., 1999), or in an isolated primitive reservoir in the lower mantle (Allègre et al., 1983; Tolstikhin and Hofmann, 2005) or even in the core (Bouhifd et al., 2013), to explain the isotopic variability observed within individual hotspot tracks.

The Juan Fernandez Islands do not show a double volcanic chain, unlike Hawaii and the other volcanic chains investigated by Huang et al. (2011). Sampling resolution
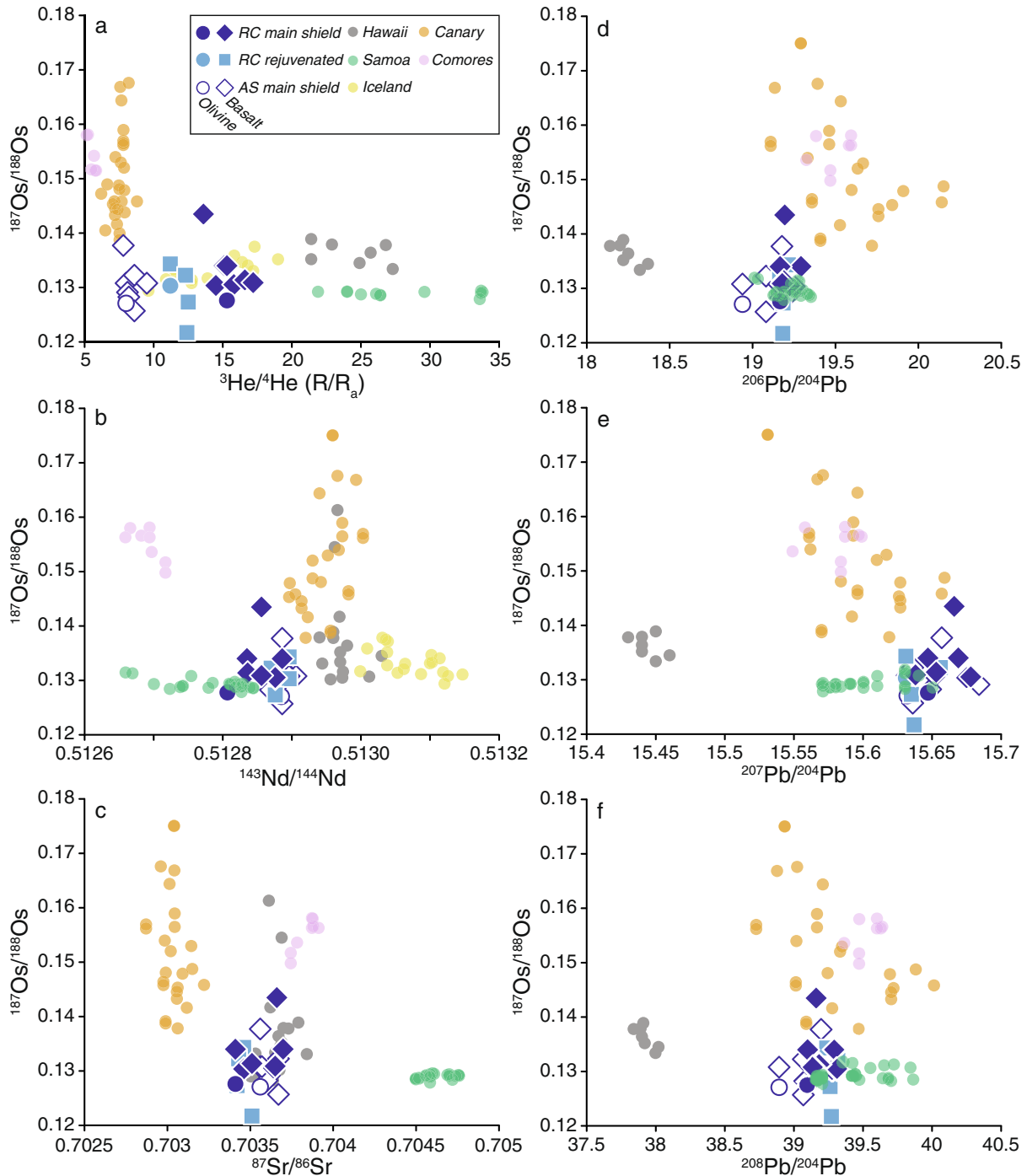
Fig. 12. Osmium isotope compositions compared with (a) $^{3}He/^{4}He$ (R/R$_a$), (b) $^{143}Nd/^{144}Nd$, (c) $^{87}Sr/^{86}Sr$, (d) $^{206}Pb/^{204}Pb$, (e) $^{207}Pb/^{204}Pb$ and (f) $^{208}Pb/^{204}Pb$ for Juan Fernandez lavas (diamonds and squares) and olivine separates (circles), and compared with lavas from Hawaii (Mukhopadhyay et al., 2003; Bryce et al., 2005; Jamais et al., 2008), the Comores Islands (Class et al., 1998, 2005, 2009), the Canary Islands (Day et al., 2010, Day & Hilton, 2011), Iceland (Brandon et al., 2007;) and Samoa (Jackson et al., 2007, Jackson & Shirey, 2011; Konter and Jackson, 2012). RC main shield = Robinson Crusoe main shield lavas and olivine; RC rejuvenated = Robinson Crusoe rejuvenated lavas and olivine; AS main shield = Alexander Selkirk main shield lavas and olivine.

on Juan Fernandez lavas does not allow us to identify two geochemical trends in the isotopic data between Robinson Crusoe and Alexander Selkirk. However, the isotopic variability in the mantle plume observed between the main

shield lavas of the two islands could be due to a variety of models including a compositionally heterogeneous mantle source, with heterogeneities being vertically stretched and rising at different rates inside the plume conduit (e.g.,

Farnetani & Hofmann, 2010), sampling of lower mantle (e.g. Allègre et al., 1983; Tolstikhin and Hofmann, 2005) and LLSVP material (e.g., Weis et al., 2011).

The origin of the isotopically depleted component in hotspots is debated: it has been proposed as (1) entrained upper mantle (e.g. Lassiter et al., 2000; Regelous et al., 2003), (2) metasomatized lithospheric mantle (e.g. Pilet et al., 2008; Sorbadere et al., 2013), (3) intrinsic to the plume (e.g. Yang et al., 2003; Mukhopadhyay et al., 2003; Frey et al., 2005; DeFelice et al., 2019) or (4) subducted ancient lithospheric mantle (Castillo, 2015; Truong et al., 2018). The Samoan depleted component is thought to be entrained depleted mantle (e.g. Konter and Jackson, 2012), whereas all the first three sources have been proposed for the depleted component in the Galapagos (e.g. Blichert-Toft and White, 2001; Saal et al., 2007) and Icelandic plumes (e.g. Fitton et al., 1997; Hanan et al., 2000; Chauvel and Hémond, 2000). For the Hawaiian lavas, the depleted component has been proposed to be an isotopically depleted component intrinsic to the plume (e.g., Yang et al., 2003; Mukhopadhyay et al., 2003; Frey et al., 2005; DeFelice et al., 2019), the lithospheric mantle (e.g. Lassiter et al., 2000) or even the Pacific DMM (e.g. Keller et al., 2000). The addition of a depleted MORB-like mantle component well explains the isotopic composition of Alexander Selkirk main shield lavas, with the isotopic signature of these lavas being consistent with sampling of FOZO and a more depleted component (Fig. 11). However, a higher contribution of this depleted component to the compositions of Alexander Selkirk lavas should produce depleted trace element patterns relative to Robinson Crusoe main shield lavas, which is not what we observe (Fig. 3). Thus, even if Alexander Selkirk main shield lavas are slightly more isotopically depleted relative to those from Robinson Crusoe, they might still sample a heterogeneous FOZO domain, possibly distinct from the DMM, to produce such trace element compositions.

5. CONCLUSIONS

We present new major-, trace- and highly siderophile-element abundances (HSE: Re, Pd, Pt, Ru, Ir, Os) and Os isotope compositions for a suite of lavas and olivine separates from the Juan Fernandez Islands. We clarify the previous grouping scheme of Farley et al. (1993) for the basalts after showing that Robinson Crusoe basanites are rejuvenated lavas. The fractionation of an assemblage of 30 modal % olivine and 1–5 modal % spinel, plus a small contribution of the primary melt from olivine melt inclusions (1–2% for both main shield lavas, up to 5% for the rejuvenated lavas), recreates HSE patterns for olivine grains in samples and also reproduces the range of HSE compositions observed in Juan Fernandez lavas, consistent with modeling of REE abundances in the olivine separates. Overall, Juan Fernandez lavas sample the convergence zone of all OIB, at the "FOZO" or "C" component. Robinson Crusoe basanite lavas represent rejuvenated volcanism dominantly from a depleted lithospheric mantle source ($^{187}Os/^{188}Os < 0.13$) polluted by high-$^3He/^4He$ from the main shield building stage of the island. Robinson Crusoe

main shield lavas sample a high-$^3He/^4He$ (>18 R_A) and enriched mantle source ($^{187}Os/^{188}Os = 0.1312$) akin to the FOZO or C component, whereas Alexander Selkrik lavas are from a dominant contribution from a depleted mantle component with low-$^3He/^4He$ (<10 R_A). Apart from their He signature, these mantle sources of the shield lavas show limited variations for the other radiogenic isotopes, and no clear variations of the HSE or trace elements, likely due to limited differences in the source composition and degree of partial melting. We propose that Robinson Crusoe form during an initial eruption stage of lavas from a primitive high-$^3He/^4He$ mantle source at ∼ 4 Ma, which also led to noble gas impregnation of the oceanic lithosphere. This first stage was followed by eruption of Alexander Selkirk lavas from a more depleted mantle source at ∼ 2 Ma. Mantle heterogeneity preserved in Juan Fernandez lavas over short timescales (<2 Ma) can impact lithospheric compositions, resulting in formation of rejuvenated lavas with unique isotopic compositions.

APPENDIX A. SUPPLEMENTARY MATERIAL

Supplementary data to this article can be found online at https://doi.org/10.1016/j.gca.2019.06.039.

REFERENCES

Abouchami W., Hofmann A. W., Galer S. J. G., Frey F. A., Eisele J. and Feigenson M. (2005) Lead isotopes reveal bilateral asymmetry and vertical continuity in the Hawaiian mantle plume. *Nature* **434**(7035), 851.

Allègre C. J., Staudacher T., Sarda P. and Kurz M. (1983) Constraints on evolution of Earth's mantle from rare gas systematics. *Nature* **303**(5920), 762.

Baker P. E., Gledhill A., Harvey P. K. and Hawkesworth C. J. (1987) Geochemical evolution of the Juan Fernandez islands, SE Pacific. *J. Geol. Soc.* **144**(6), 933–944.

Becker T. W., Kellogg J. B. and O'Connell R. J. (1999) Thermal constraints on the survival of primitive blobs in the lower mantle. *Earth Planet. Sci. Lett.* **171**(3), 351–365.

Bianco T. A., Ito G., Becker J. M. and Garcia M. O. (2005) Secondary Hawaiian volcanism formed by flexural arch decompression. *Geochem. Geophys. Geosyst.* **6**(8).

Birck J. L., Barman M. R. and Capmas F. (1997) Re-Os isotopic measurements at the femtomole level in natural samples. *Geostand. Geoanal. Res.* **21**(1), 19–27.

Bizimis M., Griselin M., Lassiter J. C., Salters V. J. and Sen G. (2007) Ancient recycled mantle lithosphere in the Hawaiian plume: osmium–hafnium isotopic evidence from peridotite mantle xenoliths. *Earth Planet. Sci. Lett.* **257**(1–2), 259–273.

Bizimis M., Salters V. J., Garcia M. O. and Norman M. D. (2013) The composition and distribution of the rejuvenated component across the Hawaiian plume: Hf-Nd-Sr-Pb isotope system-

atics of Kaula lavas and pyroxenite xenoliths. *Geochem. Geophys. Geosyst.* **14**(10), 4458–4478.

Blichert-Toft J. and White W. M. (2001) Hf isotope geochemistry of the Galapagos Islands. *Geochem. Geophys. Geosyst.* **2**(9).

Booker J., Bullard E. C. and Grasty R. L. (1967) Palaeomagnetism and age of rocks from Easter Island and Juan Fernandez. *Geophys. J. Int.* **12**(5), 469–471.

Bouhifd M. A., Jephcoat A. P., Heber V. S. and Kelley S. P. (2013) Helium in Earth's early core. *Nat. Geosci.* **6**(11), 982.

Brandon A. D. and Walker R. J. (2005) The debate over core–mantle interaction. *Earth Planet. Sci. Lett.* **232**(3–4), 211–225.

Brandon A. D., Graham D. W., Waight T. and Gautason B. (2007) ^{186}Os and ^{187}Os enrichments and high-^{3}He/^{4}He sources in the Earth's mantle: evidence from Icelandic picrites. *Geochim. Cosmochim. Acta* **71**(18), 4570–4591.

Brenan J. M., Finnigan C. F., McDonough W. F. and Homolova V. (2012) Experimental constraints on the partitioning of Ru, Rh, Ir, Pt and Pd between chromite and silicate melt: the importance of ferric iron. *Chem. Geol.* **302**, 16–32.

Bryce J. G., DePaolo D. J. and Lassiter J. C. (2005) Geochemical structure of the Hawaiian plume: Sr, Nd, and Os isotopes in the 2.8 km HSDP-2 section of Mauna Kea volcano. *Geochem. Geophys. Geosyst.* **6**(9).

Castillo P. R. (2015) The recycling of marine carbonates and sources of HIMU and FOZO ocean island basalts. *Lithos* **216**, 254–263.

Chauvel C. and Hémond C. (2000) Melting of a complete section of recycled oceanic crust: trace element and Pb isotopic evidence from Iceland. *Geochem. Geophys. Geosyst.* **1**(2).

Chen K., Walker R. J., Rudnick R. L., Gao S., Gaschnig R. M., Puchtel I. S. and Hu Z. C. (2016) Platinum-group element abundances and Re–Os isotopic systematics of the upper continental crust through time: evidence from glacial diamictites. *Geochim. Cosmochim. Acta* **191**, 1–16.

Class C., Goldstein S. L., Altherr R. and Bachèlery P. (1998) The process of plume–lithosphere interactions in the ocean basins—the case of Grande Comore. *J. Petrol.* **39**(5), 881–903.

Class C., Goldstein S. L., Stute M., Kurz M. D. and Schlosser P. (2005) Grand Comore Island: a well-constrained "low ^{3}He/^{4}-He" mantle plume. *Earth Planet. Sci. Lett.* **233**(3), 391–409.

Class C., Goldstein S. L. and Shirey S. B. (2009) Osmium isotopes in Grande Comore lavas: a new extreme among a spectrum of EM-type mantle endmembers. *Earth Planet. Sci. Lett.* **284**(1), 219–227.

Cohen A. S. and Waters F. G. (1996) Separation of osmium from geological materials by solvent extraction for analysis by thermal ionisation mass spectrometry. *Anal. Chim. Acta* **332**(2), 269–275.

Danyushevsky L. V. and Plechov P. (2011) Petrolog 3: integrated software for modeling crystallization processes. *Geochem. Geophys. Geosyst.* **12**(7).

Day J. M. D. (2013) Hotspot volcanism and highly siderophile elements. *Chem. Geol.* **341**, 50–74.

Day J. M. D. and Hilton D. R. (2011) Origin of ^{3}He/^{4}He ratios in HIMU-type basalts constrained from Canary Island lavas. *Earth Planet. Sci. Lett.* **305**(1), 226–234.

Day J. M. D., Pearson D. G., Macpherson C. G., Lowry D. and Carracedo J. C. (2010) Evidence for distinct proportions of subducted oceanic crust and lithosphere in HIMU-type mantle beneath El Hierro and La Palma, Canary Islands. *Geochimica et Cosmochimica Acta* **74**(22), 6565–6589.

Day J. M. D., Peters B. J. and Janney P. E. (2014) Oxygen isotope systematics of South African olivine melilitites and implications for HIMU mantle reservoirs. *Lithos* **202**, 76–84.

Day J. M. D., Waters C. L., Schaefer B. F., Walker R. J. and Turner S. (2016) Use of Hydrofluoric Acid Desilicification in the Determination of Highly Siderophile Element Abundances and Re-Pt-Os Isotope Systematics in Mafic-Ultramafic Rocks. *Geostand. Geoanal. Res.* **40**(1), 49–65.

Day J. M. D., Walker R. J. and Warren J. M. (2017) ^{186}Os–^{187}Os and highly siderophile element abundance systematics of the mantle revealed by abyssal peridotites and Os-rich alloys. *Geochim. Cosmochim. Acta* **200**, 232–254.

Day J. M. D., Maria-Benavides J., McCubbin F. M. and Zeigler R. A. (2018) The potential for metal contamination during Apollo lunar sample curation. *Meteorit. Planet. Sci.* **53**(6), 1283–1291.

Debaille V., Trønnes R. G., Brandon A. D., Waight T. E., Graham D. W. and Lee C. T. A. (2009) Primitive off-rift basalts from Iceland and Jan Mayen: Os-isotopic evidence for a mantle source containing enriched subcontinental lithosphere. *Geochim. Cosmochim. Acta* **73**(11), 3423–3449.

DeFelice C., Mallick S., Saal A. E. and Huang S. (2019) An isotopically depleted lower mantle component is intrinsic to the Hawaiian mantle plume. *Nat. Geosci.* **12**(6), 487.

DeMets C., Gordon R. G. and Argus D. F. (2010) Geologically current plate motions. *Geophys. J. Int.* **181**(1), 1–80.

DePaolo D. J., Bryce J. G., Dodson A., Shuster D. L. and Kennedy B. M. (2001) Isotopic evolution of Mauna Loa and the chemical structure of the Hawaiian plume. *Geochem. Geophys. Geosyst.* **2**(7).

Devey C. W., Hémond C. and Stoffers P. (2000) Metasomatic reactions between carbonated plume melts and mantle harzburgite: the evidence from Friday and Domingo Seamounts (Juan Fernandez chain, SE Pacific). *Contrib. Miner. Petrol.* **139**(1), 68–84.

Eiler J. M., Farley K. A., Valley J. W., Hauri E., Craig H., Hart S. R. and Stolper E. M. (1997) Oxygen isotope variations in ocean island basalt phenocrysts. *Geochimica et Cosmochimica Acta* **61**(11), 2281–2293.

Farley K. A., Natland J. H. and Craig H. (1992) Binary mixing of enriched and undegassed (primitive?) mantle components (He, Sr, Nd, Pb) in Samoan lavas. *Earth Planet. Sci. Lett.* **111**(1), 183–199.

Farley K. A., Basu A. R. and Craig H. (1993) He, Sr and Nd isotopic variations in lavas from the Juan Fernandez Archipelago, SE Pacific. *Contrib. Miner. Petrol.* **115**(1), 75–87.

Farnetani C. G. and Hofmann A. W. (2009) Dynamics and internal structure of a lower mantle plume conduit. *Earth Planet. Sci. Lett.* **282**(1–4), 314–322.

Farnetani C. G. and Hofmann A. W. (2010) Dynamics and internal structure of the Hawaiian plume. *Earth Planet. Sci. Lett.* **295**(1–2), 231–240.

Fitton J. G., Saunders A. D., Norry M. J., Hardarson B. S. and Taylor R. N. (1997) Thermal and chemical structure of the Iceland plume. *Earth Planet. Sci. Lett.* **153**(3–4), 197–208.

Frey F. A., Huang S., Blichert-Toft J., Regelous M. and Boyet M. (2005) Origin of depleted components in basalt related to the Hawaiian hot spot: evidence from isotopic and incompatible element ratios. *Geochem. Geophys. Geosyst.* **6**(2).

Frey F. A., Huang S., Xu G. and Jochum K. P. (2016) The geochemical components that distinguish Loa-and Kea-trend Hawaiian shield lavas. *Geochim. Cosmochim. Acta* **185**, 160–181.

Fujimaki H., Tatsumoto M. and Aoki K. I. (1984) Partition coefficients of Hf, Zr, and REE between phenocrysts and groundmasses. *J. Geophys. Res. Solid Earth* **89**(S02), B662–B672.

Garcia M. O., Rhodes J. M., Wolfe E. W., Ulrich G. E. and Ho R. A. (1992) Petrology of lavas from episodes 2–47 of the Puu O'o eruption of Kilauea Volcano, Hawaii: evaluation of magmatic processes. *Bull. Volcanol.* **55**(1–2), 1–16.

Garcia M. O., Rhodes J. M., Trusdell F. A. and Pietruszka A. J. (1996) Petrology of lavas from the Puu Oo eruption of Kilauea Volcano: III. The Kupaianaha episode (1986–1992). *Bullet. Volcanol.* **58**(5), 359–379.

Garcia M. O., Pietruszka A. J., Rhodes J. M. and Swanson K. (2000) Magmatic processes during the prolonged Pu'u'O'o eruption of Kilauea Volcano, Hawaii. *J. Petrol.* **41**(7), 967–990.

Garcia M. O., Swinnard L., Weis D., Greene A. R., Tagami T., Sano H. and Gandy C. E. (2010) Petrology, geochemistry and geochronology of Kaua'i lavas over 4·5 Myr: implications for the origin of rejuvenated volcanism and the evolution of the Hawaiian plume. *J. Petrol.* **51**(7), 1507–1540.

Garcia M. O., Weis D., Jicha B. R., Ito G. and Hanano D. (2016) Petrology and geochronology of lavas from Ka 'ula Volcano: implications for rejuvenated volcanism of the Hawaiian mantle plume. *Geochim. Cosmochim. Acta* **185**, 278–301.

Gerlach D. C., Hart S. R., Morales V. W. J. and Palacios C. (1986) Mantle heterogeneity beneath the Nazca plate: San Felix and Juan Fernandez islands. *Nature* **322**(6075), 165–169.

Graham D. W. (2002) Noble gas isotope geochemistry of mid-ocean ridge and ocean island basalts: characterization of mantle source reservoirs. *Rev. Mineral. Geochem.* **47**(1), 247–317.

Hanan B. B., Blichert-Toft J., Kingsley R. and Schilling J. G. (2000) Depleted Iceland mantle plume geochemical signature: artifact of multicomponent mixing? *Geochem. Geophys. Geosyst.* **1**(4).

Hanan B. B. and Graham D. W. (1996) Lead and helium isotope evidence from oceanic basalts for a common deep source of mantle plumes. *Science* **272**(5264), 991–995.

Harðardóttir S., Halldórsson S. A. and Hilton D. R. (2018) Spatial distribution of helium isotopes in Icelandic geothermal fluids and volcanic materials with implications for location, upwelling and evolution of the Icelandic mantle plume. *Chem. Geol.* **480**, 12–27.

Hart S. R., Hauri E. H., Oschmann L. A. and Whitehead J. A. (1992) Mantle plumes and entrainment: isotopic evidence. *Science* **256**(5056), 517–520.

Haskins E. H. and Garcia M. O. (2004) Scientific drilling reveals geochemical heterogeneity within the Ko'olau shield, Hawaii. *Contrib. Mineral. Petrol.* **147**(2), 162–188.

Hauri E. H. and Hart S. R. (1994) Constraints on melt migration from mantle plumes: a trace element study of peridotite xenoliths from Savai'i, Western Samoa. *J. Geophys. Res. Solid Earth* **99**(B12), 24301–24321.

Hilton D. R., Macpherson C. G. and Elliott T. R. (2000) Helium isotope ratios in mafic phenocrysts and geothermal fluids from La Palma, the Canary Islands (Spain): implications for HIMU mantle sources. *Geochim. Cosmochim. Acta* **64**(12), 2119–2132.

Hilton D. R., Grönvold K., Macpherson C. G. and Castillo P. R. (1999) Extreme ^{3}He/^{4}He ratios in northwest Iceland: constraining the common component in mantle plumes. *Earth Planet. Sci. Lett.* **173**(1–2), 53–60.

Hofmann A. W. (2014) Sampling mantle heterogeneity through oceanic basalts: isotopes and trace elements. *Treatise Geochem.* **3**, 67–101.

Huang S., Hall P. S. and Jackson M. G. (2011) Geochemical zoning of volcanic chains associated with Pacific hotspots. *Nat. Geosci.* **4**(12), 874.

Ireland T. J., Walker R. J. and Garcia M. O. (2009) Highly siderophile element and ^{187}Os isotope systematics of Hawaiian picrites: implications for parental melt composition and source heterogeneity. *Chem. Geol.* **260**(1), 112–128.

Jackson M. G. and Shirey S. B. (2011) Re–Os isotope systematics in Samoan shield lavas and the use of Os-isotopes in olivine phenocrysts to determine primary magmatic compositions. *Earth Planet. Sci. Lett.* **312**(1), 91–101.

Jackson M. G., Kurz M. D., Hart S. R. and Workman R. K. (2007) New Samoan lavas from Ofu Island reveal a hemispherically heterogeneous high ^{3}He/^{4}He mantle. *Earth Planet. Sci. Lett.* **264**(3), 360–374.

Jackson M. G., Hart S. R., Saal A. E., Shimizu N., Kurz M. D., Blusztajn J. S. and Skovgaard A. C. (2008) Globally elevated titanium, tantalum, and niobium (TITAN) in ocean island basalts with high ^{3}He/^{4}He. *Geochem. Geophys. Geosyst.* **9**(4).

Jackson M. G., Shirey S. B., Hauri E. H., Kurz M. D. and Rizo H. (2016) Peridotite xenoliths from the Polynesian Austral and Samoa hotspots: implications for the destruction of ancient ^{187}Os and ^{142}Nd isotopic domains and the preservation of Hadean ^{129}Xe in the modern convecting mantle. *Geochim. Cosmochim. Acta* **185**, 21–43.

Jamais M., Lassiter J. C. and Brügmann G. (2008) PGE and Os-isotopic variations in lavas from Kohala Volcano, Hawaii: constraints on PGE behavior and melt/crust interaction. *Chem. Geol.* **250**(1–4), 16–28.

Keller R. A., Fisk M. R. and White W. M. (2000) Isotopic evidence for Late Cretaceous plume–ridge interaction at the Hawaiian hotspot. *Nature* **405**(6787), 673.

Konter J. G. and Jackson M. G. (2012) Large volumes of rejuvenated volcanism in Samoa: evidence supporting a tectonic influence on late-stage volcanism. *Geochem. Geophys. Geosyst.* **13**(6).

Kurz M. D., Jenkins W. J. and Hart S. R. (1982) Helium isotopic systematics of oceanic islands and mantle heterogeneity. *Nature* **297**(5861), 43–47.

Lara L. E., Díaz-Naveas J., Reyes J., Jicha B., Orozco G., Tassara A. and Kay S. (2018a) Unraveling short-lived rejuvenated volcanism and a rapid transition from shield stage at O'Higgins Guyot, Juan Fernández Ridge, Pacific SE. *Deep Sea Res. Part I* **141**, 33–42.

Lara L. E., Reyes J. and Diaz-Naveas J. (2018b) ^{40}Ar/^{39}Ar constraints on the age progression along the Juan Fernández Ridge, SE Pacific. *Front. Earth Sci.* **6**, 194.

Lassiter J. C., Hauri E. H., Reiners P. W. and Garcia M. O. (2000) Generation of Hawaiian post-erosional lavas by melting of a mixed lherzolite/pyroxenite source. *Earth Planet. Sci. Lett.* **178**(3–4), 269–284.

Lassiter J. C. and Hauri E. H. (1998) Osmium-isotope variations in Hawaiian lavas: evidence for recycled oceanic lithosphere in the Hawaiian plume. *Earth Planet. Sci. Lett.* **164**(3), 483–496.

Maier W. D., O'Brien H., Peltonen P. and Barnes S. J. (2017) Platinum-group element contents of Karelian kimberlites: implications for the PGE budget of the sub-continental lithospheric mantle. *Geochim. Cosmochim. Acta* **216**, 358–371.

Maier W. D., Peltonen P., McDonald I., Barnes S. J., Barnes S. J., Hatton C. and Viljoen F. (2012) The concentration of platinum-group elements and gold in southern African and Karelian kimberlite-hosted mantle xenoliths: implications for the noble metal content of the Earth's mantle. *Chem. Geol.* **302**, 119–135.

McDonough W. F. and Sun S. S. (1995) The composition of the Earth. *Chem. Geol.* **120**(3–4), 223–253.

Meisel T., Walker R. J., Irving A. J. and Lorand J. P. (2001) Osmium isotopic compositions of mantle xenoliths: a global perspective. *Geochim. Cosmochim. Acta* **65**(8), 1311–1323.

Mukhopadhyay S., Lassiter J. C., Farley K. A. and Bogue S. W. (2003) Geochemistry of Kauai shield-stage lavas: implications for the chemical evolution of the Hawaiian plume. *Geochem. Geophys. Geosyst.* **4**(1).

Nagasawa H., Schreiber H. D. and Morris R. V. (1980) Experimental mineral/liquid partition coefficients of the rare earth elements (REE), Sc and Sr for perovskite, spinel and melilite. *Earth Planet. Sci. Lett.* **46**(3), 431–437.

Natland J. H. (2003) Capture of helium and other volatiles during the growth of olivine phenocrysts in picritic basalts from the Juan Fernandez Islands. *J. Petrol.* **44**(3), 421–456.

Peters B. J. and Day J. M. D. (2014) Assessment of relative Ti, Ta, and Nb (TITAN) enrichments in ocean island basalts. *Geochem. Geophys. Geosyst.* **15**(11), 4424–4444.

Peters B. J., Day J. M. D. and Taylor L. A. (2016) Early mantle heterogeneities in the Réunion hotspot source inferred from highly siderophile elements in cumulate xenoliths. *Earth Planet. Sci. Lett.* **448**, 150–160.

Phillips E. H., Sims K. W., Sherrod D. R., Salters V. J., Blusztajn J. and Dulai H. (2016) Isotopic constraints on the genesis and evolution of basanitic lavas at Haleakala, Island of Maui, Hawaii. *Geochimica et Cosmochimica Acta* **195**, 201–225.

Pilet S., Baker M. B. and Stolper E. M. (2008) Metasomatized lithosphere and the origin of alkaline lavas. *Science* **320**(5878), 916–919.

Puchtel I. S. and Humayun M. (2001) Platinum group element fractionation in a komatiitic basalt lava lake. *Geochim. Cosmochim. Acta* **65**(17), 2979–2993.

Regelous M., Hofmann A. W., Abouchami W. and Galer S. J. G. (2003) Geochemistry of lavas from the Emperor Seamounts, and the geochemical evolution of Hawaiian magmatism from 85 to 42 Ma. *J. Petrol.* **44**(1), 113–140.

Rehkämper M., Halliday A. N., Barfod D., Fitton J. G. and Dawson J. B. (1997) Platinum-group element abundance patterns in different mantle environments. *Science* **278**(5343), 1595–1598.

Reyes J., Lara L. E. and Morata D. (2017) Contrasting P-T paths of shield and rejuvenated volcanism at Robinson Crusoe Island, Juan Fernández Ridge, SE Pacific. *J. Volcanol. Geoth. Res.* **341**, 242–254.

Righter K., Campbell A. J., Humayun M. and Hervig R. L. (2004) Partitioning of Ru, Rh, Pd, Re, Ir, and Au between Cr-bearing spinel, olivine, pyroxene and silicate melts1. *Geochim. Cosmochim. Acta* **68**(4), 867–880.

Rodrigo C. and Lara L. E. (2014) *Plate tectonics and the origin of the Juan Fernández Ridge: analysis of bathymetry and magnetic patterns*.

Roy-Barman M. and Allègre C. J. (1995) [187]Os/[186]Os in oceanic island basalts: tracing oceanic crust recycling in the mantle. *Earth Planet. Sci. Lett.* **129**(1–4), 145–161.

Saal A. E., Kurz M. D., Hart S. R., Blusztajn J. S., Blichert-Toft J., Liang Y. and Geist D. J. (2007) The role of lithospheric gabbros on the composition of Galapagos lavas. *Earth Planet. Sci. Lett.* **257**(3–4), 391–406.

Savard D., Barnes S. J. and Meisel T. (2010) Comparison between nickel-sulfur fire assay Te co-precipitation and isotope dilution with high-pressure asher acid digestion for the determination of platinum-group elements, rhenium and gold. *Geostand. Geoanal. Res.* **34**(3), 281–291.

Selby D., Creaser R. A., Stein H. J., Markey R. J. and Hannah J. L. (2007) Assessment of the [187]Re decay constant by cross calibration of Re–Os molybdenite and U-Pb zircon chronometers in magmatic ore systems. *Geochim. Cosmochim. Acta* **71**(8), 1999–2013.

Sen I. S., Bizimis M., Sen G. and Huang S. (2011) A radiogenic Os component in the oceanic lithosphere? Constraints from Hawaiian pyroxenite xenoliths. *Geochim. Cosmochim. Acta* **75**(17), 4899–4916.

Sinton J. M., Eason D. E. and Duncan R. A. (2017) Volcanic evolution of Moloka 'i, Hawai 'i: implications for the shield to postshield transition in Hawaiian volcanoes. *J. Volcanol. Geoth. Res.* **340**, 30–51.

Sorbadere F., Médard E., Laporte D. and Schiano P. (2013) Experimental melting of hydrous peridotite–pyroxenite mixed sources: constraints on the genesis of silica-undersaturated magmas beneath volcanic arcs. *Earth Planet. Sci. Lett.* **384**, 42–56.

Stuessy T. F., Foland K. A., Sutter J. F. and Silva M. O. (1984) Botanical and geological significance of potassium-argon dates from the Juan Fernandez Islands. *Science* **225**, 49–52.

Tolstikhin I. and Hofmann A. W. (2005) Early crust on top of the Earth's core. *Phys. Earth Planet. Inter.* **148**(2–4), 109–130.

Truong T. B., Castillo P. R., Hilton D. R. and Day J. M. D. (2018) The trace element and Sr-Nd-Pb isotope geochemistry of Juan Fernandez lavas reveal variable contributions from a high-[3]-He/[4]He mantle plume. *Chem. Geol.* **476**, 280–291.

Valbracht P. J., Staudacher T., Malahoff A. and Allègre C. J. (1997) Noble gas systematics of deep rift zone glasses from Loihi Seamount, Hawaii. *Earth Planet. Sci. Lett.* **150**(3–4), 399–411.

Weis D., Garcia M. O., Rhodes J. M., Jellinek M. and Scoates J. S. (2011) Role of the deep mantle in generating the compositional asymmetry of the Hawaiian mantle plume. *Nat. Geosci.* **4**(12), 831.

Widom E., Hoernle K. A., Shirey S. B. and Schmincke H. U. (1999) Os isotope systematics in the Canary Islands and Madeira: lithospheric contamination and mantle plume signatures. *J. Petrol.* **40**(2), 279–296.

Yang H. J., Frey F. A. and Clague D. A. (2003) Constraints on the source components of lavas forming the Hawaiian North Arch and Honolulu Volcanics. *J. Petrol.* **44**(4), 603–627.

Associate editor: Shichun Huang